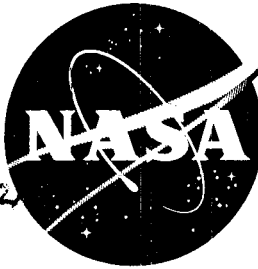


34/

CONFIDENTIAL NASA TM X-440

Classification changed to declassified  
effective 1 April 1961 by  
authority of NASA GPO by  
J. J. Carroll



# TECHNICAL MEMORANDUM

X-440

AN INVESTIGATION AT SUBSONIC SPEEDS OF  
THE LONGITUDINAL AERODYNAMIC CHARACTERISTICS AT  
ANGLES OF ATTACK FROM  $-4^{\circ}$  TO  $100^{\circ}$  OF DELTA-WING  
REENTRY CONFIGURATIONS HAVING VERTICALLY  
DISPLACED AND CAMBERED WING-TIP PANELS

By Bernard Spencer, Jr.

Langley Research Center  
Langley Field, Va.

UNCLASSIFIED DOCUMENT - PUBLIC RELEASE

This material contains information affecting the national defense of the United States within the meaning of the espionage laws, Title 18, U.S.C., Secs. 793 and 794, the transmission or revelation of its contents in any manner to an unauthorized person is prohibited by law.

NATIONAL AERONAUTICS AND SPACE ADMINISTRATION  
WASHINGTON

February 1961

CONFIDENTIAL

U N C L A S S I F I E D

CONFIDENTIAL

NATIONAL AERONAUTICS AND SPACE ADMINISTRATION

TECHNICAL MEMORANDUM X-440

AN INVESTIGATION AT SUBSONIC SPEEDS OF  
THE LONGITUDINAL AERODYNAMIC CHARACTERISTICS AT  
ANGLES OF ATTACK FROM  $-4^{\circ}$  TO  $100^{\circ}$  OF DELTA-WING  
REENTRY CONFIGURATIONS HAVING VERTICALLY  
DISPLACED AND CAMBERED WING-TIP PANELS\*

By Bernard Spencer, Jr.

SUMMARY

An investigation was made in the Langley high-speed 7- by 10-foot tunnel at Mach numbers from 0.40 to 0.80 to determine the longitudinal stability and control characteristics associated with a  $73^{\circ}$  delta-wing configuration having cambered and vertically displaced wing-tip panels. The use of trailing-edge flaps on the wing-tip panels as a method of providing longitudinal control in a normal range of angles of attack ( $-2^{\circ}$  to  $50^{\circ}$ ) and the use of fuselage nose tabs as a means of providing trim or control at high angles of attack ( $100^{\circ}$  to  $60^{\circ}$ ) were studied. A cranked-delta-wing configuration was also tested.

Unfolding fuselage nose tabs on the  $73^{\circ}$  delta-wing configuration indicated feasible trim control for maintaining the configuration at an angle of attack near  $90^{\circ}$ .

The use of a cranked-leading-edge wing having the basic vertically displaced and cambered wing-tip panels indicated a fairly linear variation of pitching moment with angle of attack and reduced the degree of pitch-up noted for the basic  $73^{\circ}$  delta wing having the same wing-tip panels.

INTRODUCTION

Present interest in winged reentry vehicles which utilize high-drag reentry for heat energy dissipation while maintaining some lift for

---

\*Title, Unclassified.

CONFIDENTIAL

trajectory control has resulted in investigations by the National Aeronautics and Space Administration relative to the various planforms and controls that may be suitable for this type configuration. These studies have included several delta-wing planforms which utilized wing-tip panels that unfolded into the airstream as an aid in transition from the high-drag phase of reentry (angles of attack near  $90^\circ$ ) to a normal glide attitude. (See refs. 1 to 7.) From information provided by these studies of the effect of diverse-wing and wing-tip-panel geometry at subsonic speeds (ref. 4), a  $73^\circ$  delta-wing configuration, which appeared to provide adequate longitudinal stability characteristics in the glide attitude, evolved. (See ref. 8.)

From a lateral stability and control standpoint, however, these configurations could possibly present a problem in that the volume of the vertical tail was low, due to a short coupled moment arm from center of gravity to the center of pressure of the vertical tail.

The present investigation was initiated to provide information on the longitudinal stability and control characteristics associated with a  $73^\circ$  delta-wing configuration having vertically displaced wing-tip panels employing camber and a higher aspect ratio than those previously tested. Trailing-edge controls located on the wing-tip panels were also employed to provide longitudinal control in the glide region, and fuselage nose tabs were used as an aid in control at angles of attack near  $90^\circ$ . Another configuration having a cranked or broken-sweep delta wing was also tested.

# SYMBOLS

All data presented in this paper are referenced to the wind-axis system, and all coefficients are nondimensionalized with respect to the basic  $73^\circ$  delta wing. The moment-reference location (fig. 1) was at the centroid of area of this wing which corresponds to the theoretical center-of-pressure location at hypersonic speeds at an angle of attack of  $90^\circ$ .

$C_D$  drag coefficient,  $\frac{\text{Drag}}{qS}$

$C_L$  lift coefficient,  $\frac{\text{Lift}}{qS}$

$C_m$  pitching-moment coefficient,  $\frac{\text{Pitching moment}}{qS\bar{c}}$

U N C L A S S I F I E D

CONFIDENTIAL

3

$\bar{c}$	wing mean aerodynamic chord, wing-tip panels off, ft
M	Mach number
q	dynamic pressure, lb/sq ft
S	wing area, wing-tip panels off, sq ft
$\alpha$	angle of attack, deg
$\Gamma_h$	wing-tip-panel deflection angle from position perpendicular to wing-chord plane (fig. 2), deg
$\delta_c$	control-tab deflection angle from position perpendicular to wing-chord plane (fig. 2), deg
$\delta_f$	wing-tip-panel flap deflection angle (fig. 2), deg

Model component designations:

C <sub>1</sub>	fuselage nose control tab having diameter of 3.14 in.
C <sub>2</sub>	fuselage nose control tab having diameter of 6.28 in.
H <sub>1</sub>	cambered wing-tip panels having area of approximately 0.37S and an aspect ratio of 1.45
H <sub>2</sub>	cambered wing-tip panels having area of approximately 0.23S and an aspect ratio of 0.81
W <sub>1</sub>	basic 73° delta wing (without wing-tip panels)
W <sub>2</sub>	cranked delta wing (without wing-tip panels)

MODELS

The basic delta wing W<sub>1</sub> used in this investigation had a leading-edge sweep of 73° and was of flat-plate airfoil section with a rounded leading edge and blunt trailing edge. (See fig. 1(a).) The cambered wing-tip panel H<sub>1</sub> was displaced vertically 2.15 inches from the lower surface of the wing to the trailing edge of the panel and was constructed to approximate an NACA 6306 section. The wing-tip panels had a leading-edge sweep of 5.83°, an area of approximately 0.37S, and a taper ratio of 0.76.

CONFIDENTIAL

031715391040

4

CONFIDENTIAL

A smaller cambered wing-tip panel  $H_2$ , which had a total area equal to approximately 0.23S and was formed by clipping the wing-tip panel  $H_1$  by approximately 41 percent, was also tested. (See fig. 1(b).) The vertical fin used to displace the wing-tip panel was of 0.25-inch flat-plate section with a wedged leading edge and a beveled trailing edge.

The cranked wing  $W_2$  had an initial leading-edge sweep of  $67^\circ$ , extending 4.70 inches rearward of the wing apex at which point the leading-edge sweep was increased to  $77^\circ$ . The tip chord, span, and root chord of this wing were the same as those of the basic  $73^\circ$  wing  $W_1$ , and both wings had flat-plate sections.

Trailing-edge flaps located on the wing-tip panels were used for longitudinal control and could be preset by brackets of angles of  $0^\circ$ ,  $-10^\circ$ ,  $-20^\circ$ , and  $-30^\circ$ . The location and size of these flaps are presented in figures 1(a) and 1(b) for the wing-tip panels tested.

A fuselage nose control tab  $C_1$  having flat-plate section and circular planform was located near the wing apex. A second leading-edge extension  $C_2$  having twice the diameter of  $C_1$  and similar in planform and section was also used.

#### TESTS AND CORRECTIONS

Tests were made in the Langley high-speed 7- by 10-foot tunnel for a Mach number range from 0.40 to 0.80 corresponding to a Reynolds number range from approximately  $2.6 \times 10^6$  to  $4.6 \times 10^6$  based on the mean aerodynamic chord of the basic  $73^\circ$  delta wing alone. The models were tested through an angle-of-attack range from  $-4^\circ$  to  $100^\circ$  for all test Mach numbers. The sting-support arrangement with the basic wing and wing-tip panels for the tests at low angles of attack and the tests at high angles of attack is shown in figure 3.

Jet-boundary corrections determined by the methods of reference 9 and blockage corrections determined by the methods of reference 10 were found to be negligible because of the small size of the models relative to the tunnel dimensions and, therefore, were not applied to the data. The angle of attack has been corrected for deflection of the sting-support system under load.

CONFIDENTIAL

## RESULTS AND DISCUSSION

In this section the results are briefly presented and only the more pertinent observations are discussed.

The effects of deflecting the basic wing-tip panels on the longitudinal stability and control characteristics of the basic delta-wing configuration  $W_1H_1$  in the high-angle attitude ( $\delta_c = 0^\circ$ ;  $\delta_f = 0^\circ$ ) are presented in figure 4. Tests were begun with the model at an angle of attack of approximately  $100^\circ$  to simulate the attitude range of the actual configuration in transition. Essentially no variation in pitching-moment coefficient is produced by unfolding the wing-tip panels between  $\Gamma_h = 0^\circ$  and  $\Gamma_h = 45^\circ$  at an angle of attack of  $90^\circ$ . Reference 8 indicated the same effects for the  $73^\circ$  delta wing having wing-tip panels located in the chord plane of the wing.

Figure 5 presents the effects of deflecting the basic fuselage nose control tab on the longitudinal stability and control characteristics of the basic  $73^\circ$  delta-wing configuration  $W_1H_1C_1$  in the high-angle attitude ( $\delta_f = 0^\circ$ ;  $\Gamma_h = 0^\circ$ ). This control produces trim for an angle-of-attack range of approximately  $10^\circ$  at the highest test Mach number of 0.80.

Since the trim produced by deflection of the fuselage nose control tab  $C_1$  was for an angle-of-attack range of only approximately  $10^\circ$ , the planform area of the nose tab was increased (configuration  $W_1H_1C_2$ ;  $\delta_f = 0^\circ$ ;  $\Gamma_h = 0^\circ$ ) and compared with the basic fuselage nose tab (configuration  $W_1H_1C_1$ ;  $\delta_f = 0^\circ$ ;  $\Gamma_h = 0^\circ$ ) at  $\delta_c = 90^\circ$  in figure 6. Although the increase in planform area was excessive, it may be seen that a considerable range of trim may be produced at angles of attack near  $90^\circ$  by use of the proper size fuselage nose tab. The effects of the planform and size of the fuselage nose tab of a configuration having a similar wing planform at supersonic speeds may be seen in reference 5.

Figure 7 presents glide or landing-attitude results of the deflection of the trailing-edge flap of the basic wing-tip panel (configuration  $W_1H_1$ ;  $\Gamma_h = 90^\circ$ ; nose control off), and figure 8 presents the results of similar tests with the modified wing-tip panel (configuration  $W_1H_2$ ;  $\Gamma_h = 90^\circ$ ; nose control off). Although a wide range of low-angle trim is produced by deflection of the flap of the basic wing-tip panel, an earlier reversal in pitching-moment variation with angle of attack was noted as compared to the wing-tip panel located in the wing-chord plane for the configuration of reference 8. The pitch-up associated with this wing-tip panel  $H_1$  is somewhat reduced by use of the modified wing-tip panel  $H_2$  planform (fig. 8(c)), although a penalty in the range of trim

is realized. Figure 9 presents the results of the addition of the basic wing-tip panel and the modified wing-tip panel to the basic  $73^\circ$  delta wing.

Figure 10 presents a comparison of the longitudinal stability characteristics of the  $73^\circ$  delta wing and the cranked delta wing with and without the basic wing-tip panels on. A more linear variation of pitching moment with angle of attack is noted for the cranked wing with the displaced wing-tip panels than for the basic wing with the displaced wing-tip panels. It may be noted that large reductions in the degree of pitch-up associated with the  $73^\circ$  wing having the basic wing-tip panels result from use of the cranked wing having the same wing-tip panels throughout the Mach number range tested.

### CONCLUSIONS

An investigation was made in the Langley high-speed 7- by 10-foot tunnel at Mach numbers from 0.40 to 0.80 to determine the longitudinal stability and control characteristics associated with a  $73^\circ$  delta-wing configuration having cambered and displaced wing-tip panels for control in a normal range of angles of attack ( $-2^\circ$  to  $50^\circ$ ) and fuselage nose tabs for control at high angles of attack ( $100^\circ$  to  $60^\circ$ ). A cranked delta-wing configuration was also tested in an effort to improve the longitudinal stability of the wing-alone configuration. The results of the investigation lead to the following conclusions:

1. Unfolding fuselage nose tabs on the  $73^\circ$  delta-wing configuration indicated feasible trim control for maintaining the configuration at angles of attack near  $90^\circ$  for reentry.
2. The use of a cranked-leading-edge wing having the basic vertically displaced and cambered wing-tip panels indicated a fairly linear variation of pitching moment with angle of attack and reduced the degree of pitch-up noted for the basic  $73^\circ$  delta wing having the same wing-tip panels, in the normal range of angles of attack.

Langley Research Center,  
National Aeronautics and Space Administration,  
Langley Field, Va., October 17, 1960.

# REFERENCES

1. Paulson, John W.: Low-Speed Static Stability Characteristics of Two Configurations Suitable for Lifting Reentry From Satellite Orbit. NASA MEMO 10-22-58L, 1958.
2. Paulson, John W., and Shanks, Robert E.: Investigation of Low-Subsonic Flight Characteristics of a Model of a Flat-Bottom Hypersonic Boost-Glide Configuration Having a  $78^\circ$  Delta Wing. NASA TM X-201, 1959.
3. Petynia, William W.: Model Investigation of Water Landings of a Winged Reentry Configuration Having Outboard Folding Wing Panels. NASA TM X-62, 1959.
4. Spencer, Bernard, Jr.: High-Subsonic-Speed Investigation of the Static Longitudinal Aerodynamic Characteristics of Several Delta-Wing Configurations for Angles of Attack From  $0^\circ$  to  $90^\circ$ . NASA TM X-168, 1959.
5. Foster, Gerald V.: Exploratory Investigation at Mach Number of 2.01 of the Longitudinal Stability and Control Characteristics of a Winged Reentry Configuration. NASA TM X-178, 1959.
6. Fournier, Paul G.: Wind-Tunnel Investigation at High Subsonic Speed of the Static Longitudinal Stability Characteristics of a Winged Reentry Vehicle Having a Large Negatively Deflected Flap-Type Control Surface. NASA TM X-179, 1959.
7. Ware, George M.: Low-Subsonic-Speed Static Longitudinal Stability and Control Characteristics of a Winged Reentry-Vehicle Configuration Having Wingtip Panels That Fold up for High-Drag Reentry. NASA TM X-227, 1960.
8. Spencer, Bernard, Jr.: An Investigation at Subsonic Speeds of Aerodynamic Characteristics at Angles of Attack From  $-4^\circ$  to  $100^\circ$  of a Delta-Wing Reentry Configuration Having Folding Wingtip Panels. NASA TM X-288, 1960.
9. Gillis, Clarence L., Polhamus, Edward C., and Gray, Joseph L., Jr.: Charts for Determining Jet-Boundary Corrections for Complete Models in 7- by 10-Foot Closed Rectangular Wind Tunnels. NACA WR L-123, 1945. (Formerly NACA ARR L5G31.)
10. Herriot, John G.: Blockage Corrections for Three-Dimensional-Flow Closed-Throat Wind Tunnels, With Consideration of the Effect of Compressibility. NACA Rep. 995, 1950. (Supersedes NACA RM A7B28.)



TABLE I

GEOMETRIC CHARACTERISTICS OF WINGS

Basic wing,  $W_1$ :

Root chord, in. . . . .	17.40
Tip chord, in. . . . .	5.15
Span, in. . . . .	7.78
Mean aerodynamic chord, in. . . . .	12.36
Area, sq ft . . . . .	0.6091
Aspect ratio . . . . .	0.69
Taper ratio . . . . .	0.29
Airfoil section . . . . .	Flat plate
Leading-edge sweep angle, deg . . . . .	73

Cranked wing,  $W_2$ :

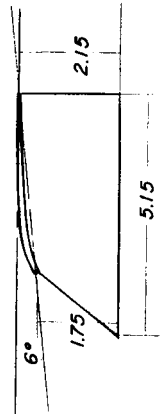
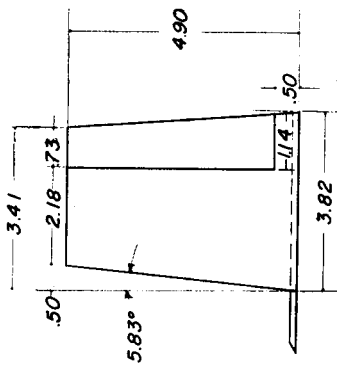
Root chord, in. . . . .	17.40
Tip chord, in. . . . .	5.15
Span, in. . . . .	7.78
Mean aerodynamic chord, in. . . . .	12.36
Area, sq ft . . . . .	0.6098
Aspect ratio . . . . .	0.69
Taper ratio . . . . .	0.29
Airfoil section . . . . .	Flat plate
Initial leading-edge sweep angle, deg . . . . .	67
Leading-edge sweep angle, 4.70 inches rearward of wing apex, deg . . . . .	77

Basic wing-tip panel,  $H_1$ :

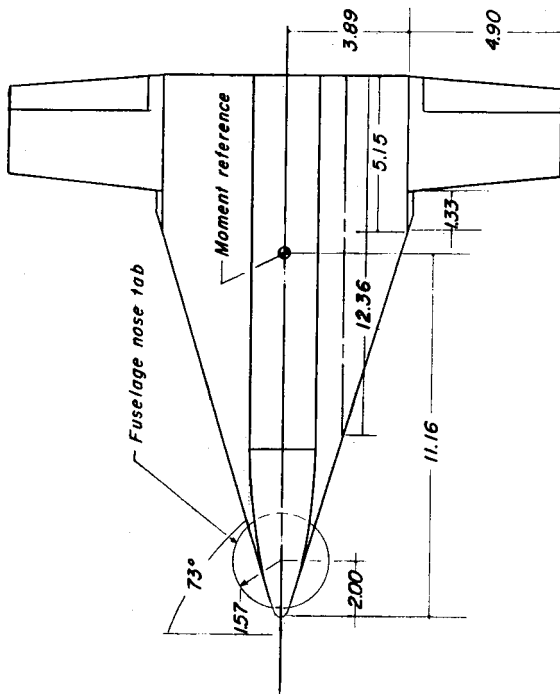
Root chord, in. . . . .	3.82
Tip chord, in. . . . .	2.91
Span (one panel), in. . . . .	4.90
Area (one panel), sq ft . . . . .	0.11
Aspect ratio . . . . .	1.45
Taper ratio . . . . .	0.76
Airfoil section (approx.) . . . . .	NACA 6306
Leading-edge sweep angle, deg . . . . .	5.83

Modified wing-tip panel,  $H_2$ :

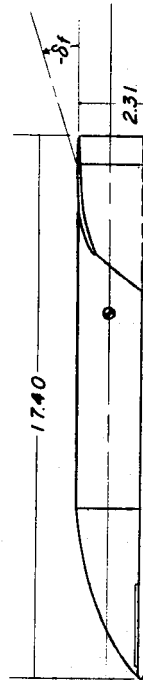
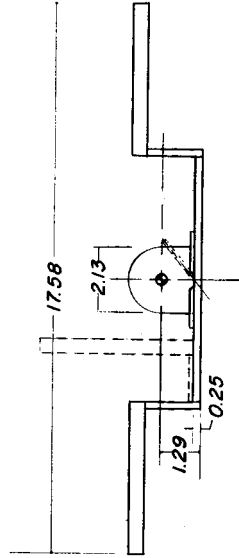
Root chord, in. . . . .	3.82
Tip chord, in. . . . .	3.28
Span (one panel), in. . . . .	2.90
Area (one panel), sq ft . . . . .	0.07
Aspect ratio . . . . .	0.81
Taper ratio . . . . .	0.86
Airfoil section . . . . .	NACA 6306
Leading-edge sweep angle, deg . . . . .	5.83



Basic displaced and cambered panel,  $H_i$   
(Approximate NACA 6306 section)

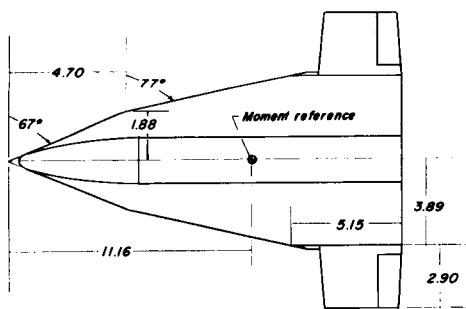


Basic configuration,  $W, H, C_l$

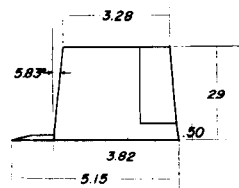


(a) Basic wing, basic displaced and cambered wing-tip panel, and fuselage control tab.

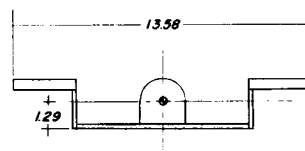
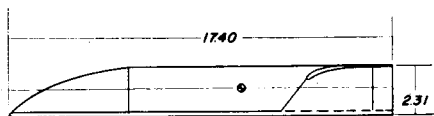
Figure 1.- Geometric characteristics of models used in this investigation. All dimensions are in inches.



*Cranked-wing configuration,  $W_2 H_2$*

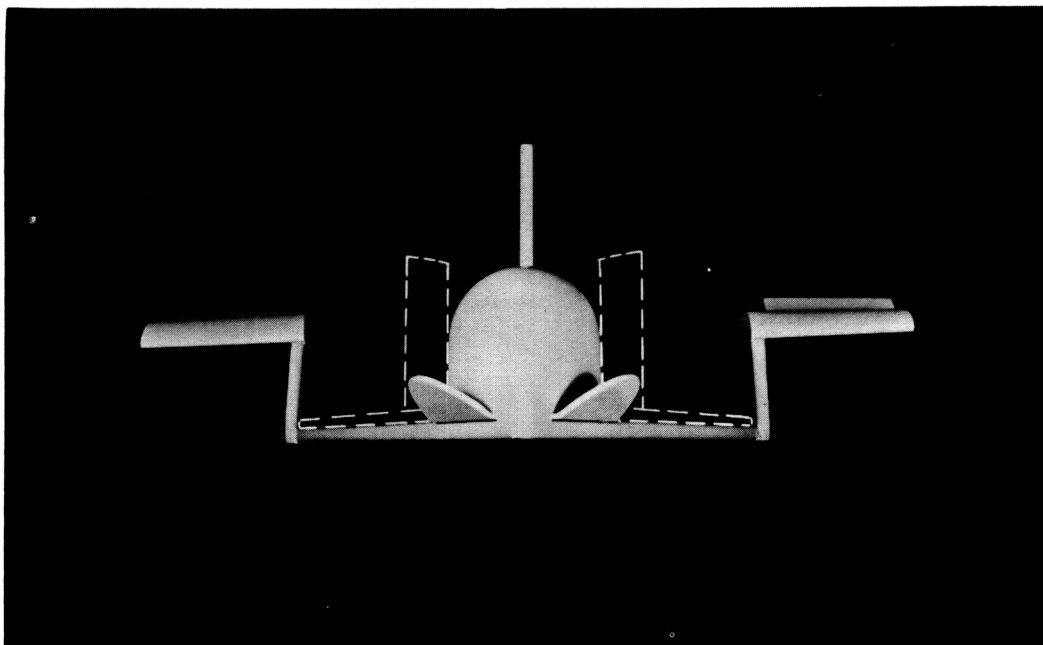


*Modified displaced and cambered panel,  $H_2$   
(Approximate NACA 6306 section)*

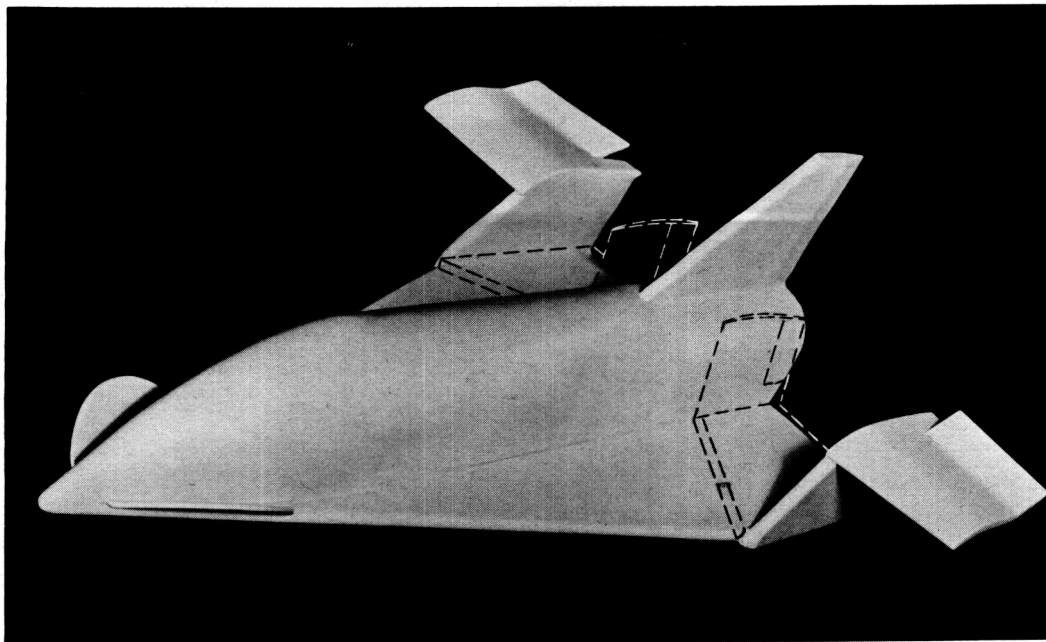


(b) Cranked wing and modified displaced and cambered wing-tip panel.

Figure 1.- Concluded.



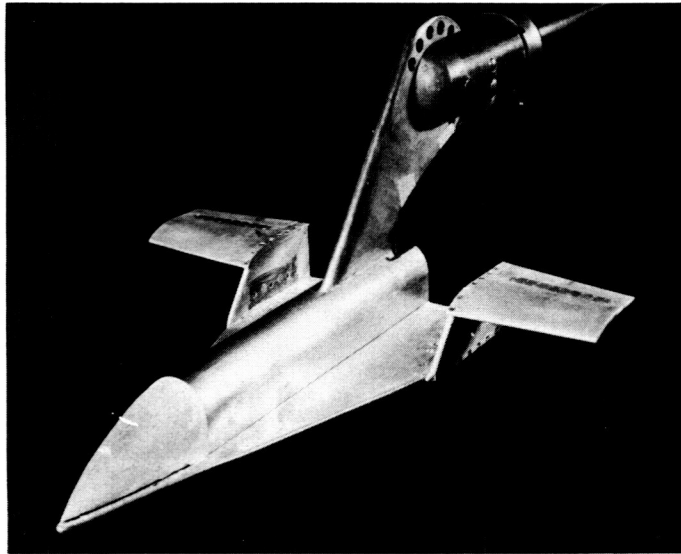
(a) Front view.



(b) Three-quarter view.

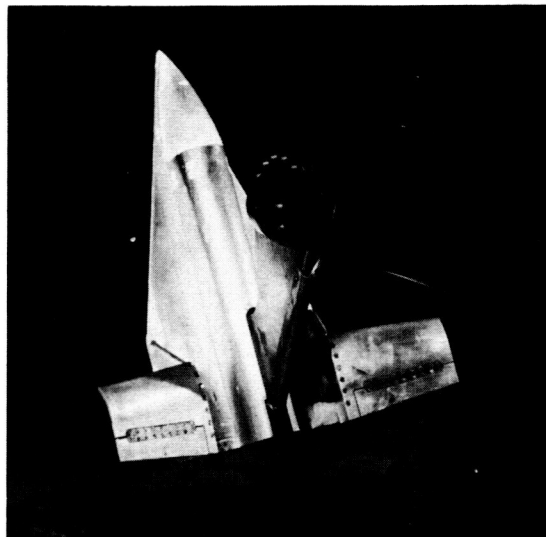
L-60-5576

Figure 2.- Photographs of model  $W_1H_2C_1$  showing control-surface deflections  $\Gamma_h = 0^\circ$  (broken line);  $\delta_f = -10^\circ$ ;  $\delta_c = 45^\circ$ .



L-59-3159

- (a) Mounting-strut arrangement for tests at normal angles of attack with basic wing and wing-tip panels  $W_1H_1$  shown.



L-59-3162

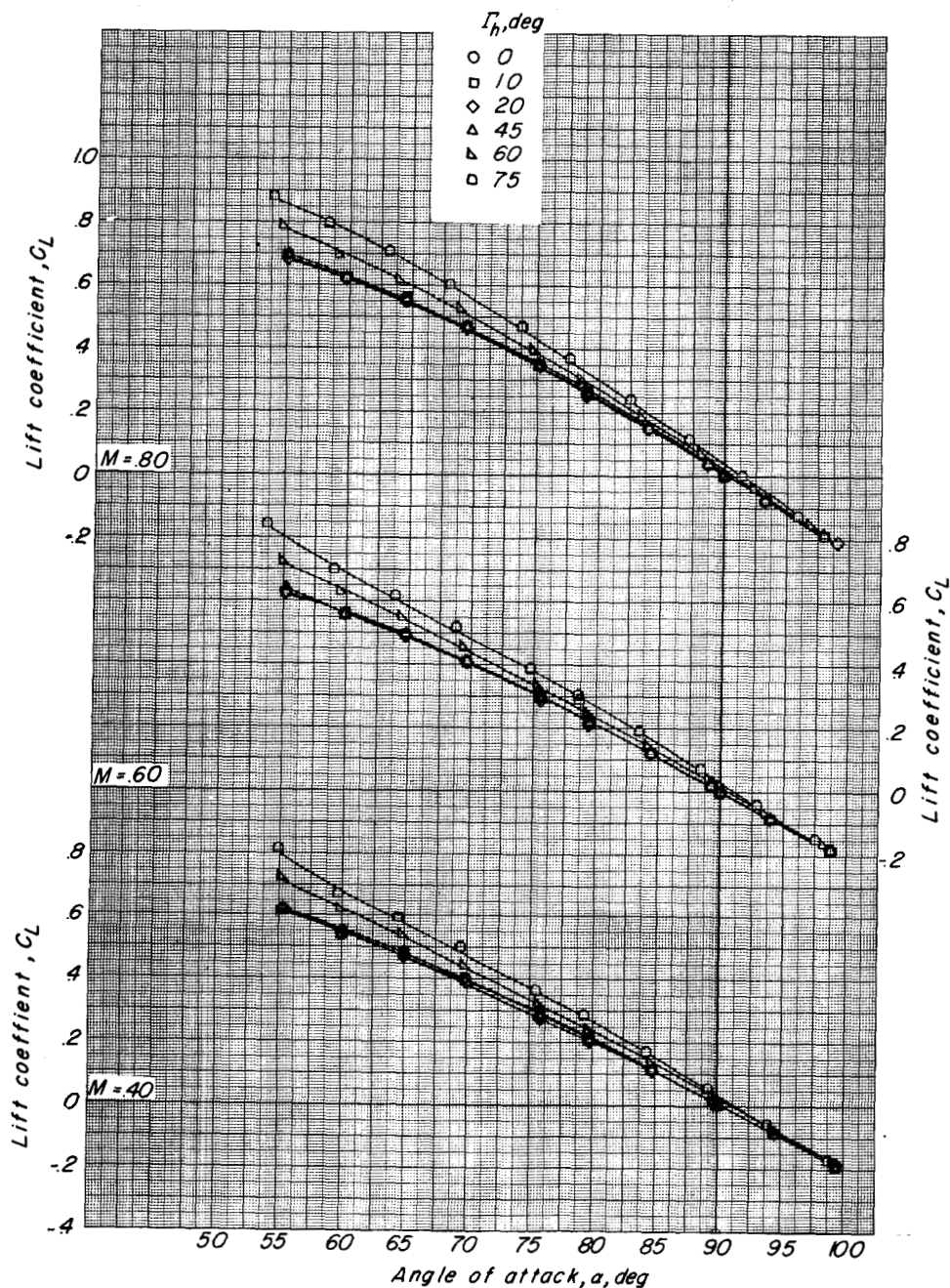
- (b) Mounting-strut arrangement for tests at high angles of attack with basic wing and wing-tip panels  $W_1H_1$  shown.

Figure 3.- Model mounting arrangement for high- and normal-attitude testing.

UNCLASSIFIED

CONFIDENTIAL

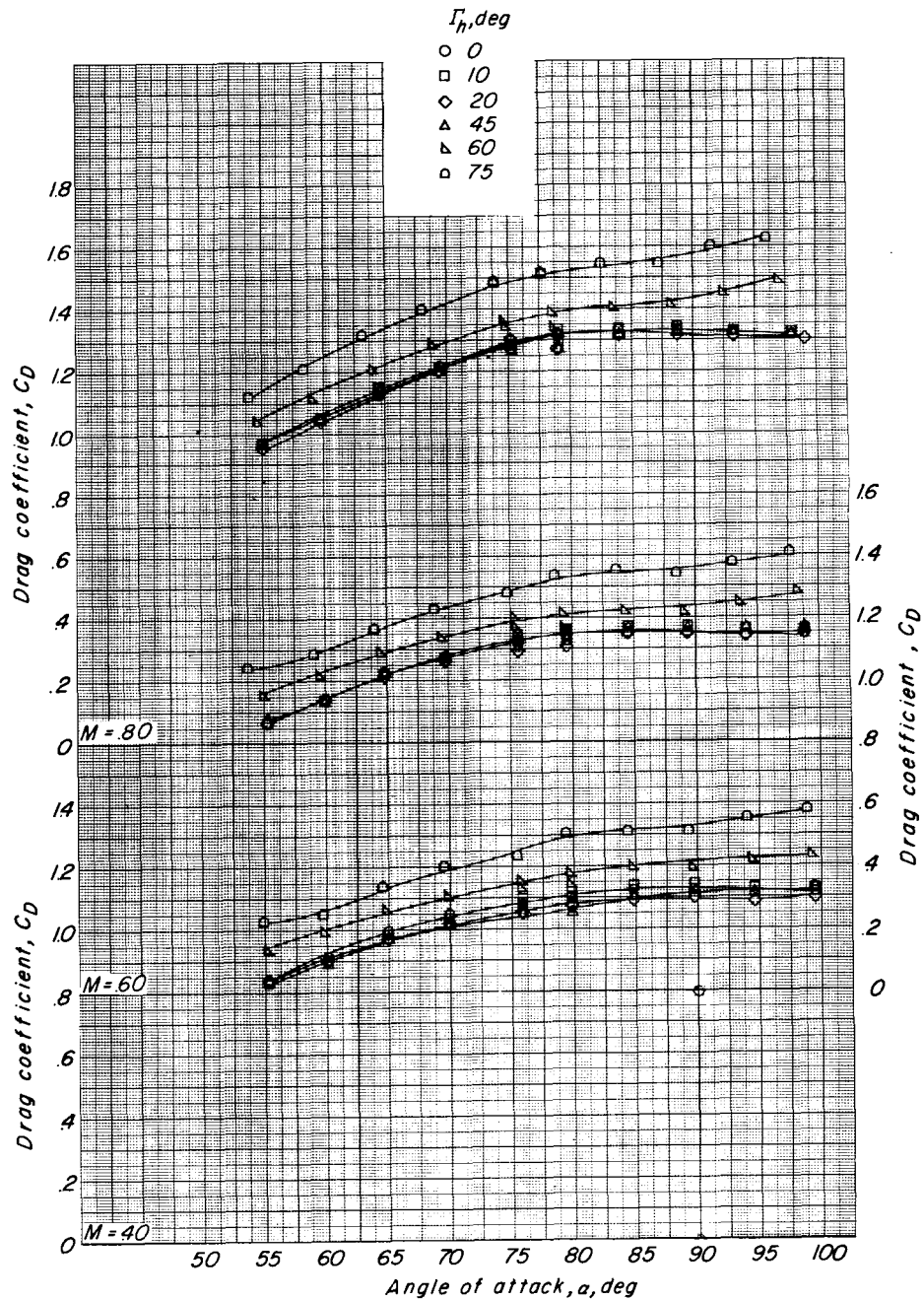
13



(a) Variation of lift coefficient with angle of attack.

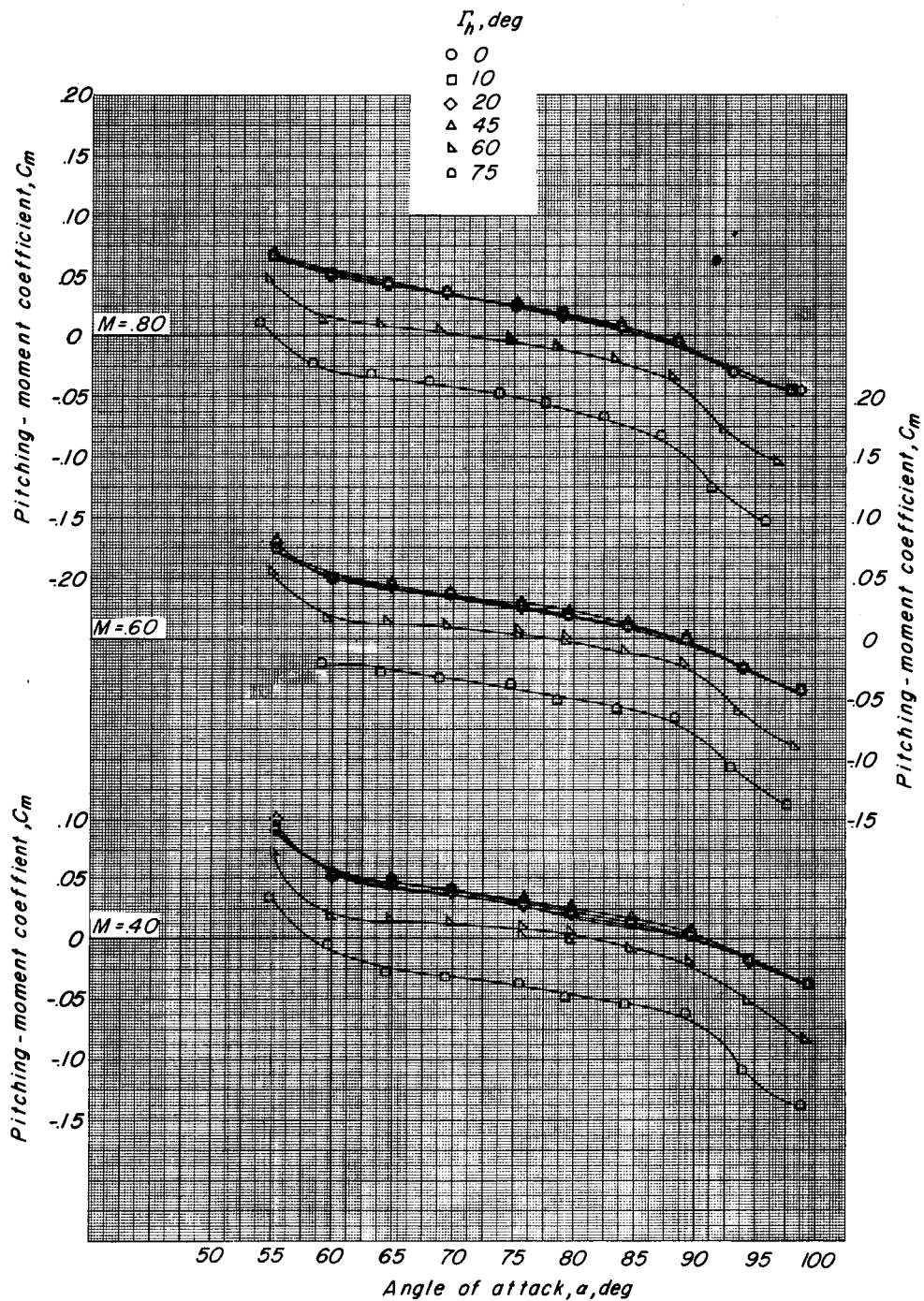
Figure 4.- Effects of deflecting the basic wing-tip panels on the longitudinal stability and control characteristics of the basic  $73^\circ$  delta-wing configuration  $W_1H_1$ .  $\delta_c = 0^\circ$ ;  $\delta_f = 0^\circ$ .

CONFIDENTIAL



(b) Variation of drag coefficient with angle of attack.

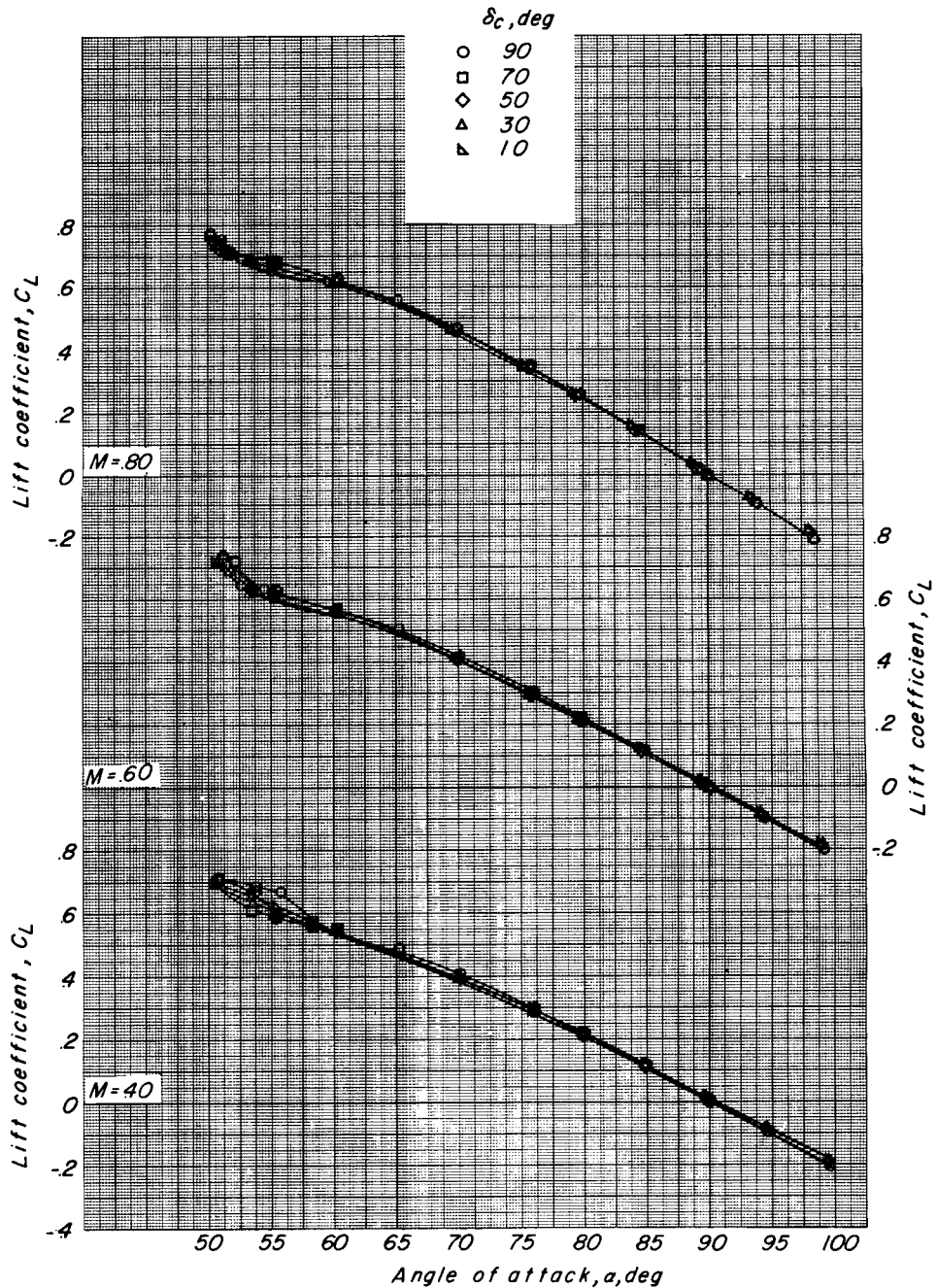
Figure 4.- Continued.



(c) Variation of pitching-moment coefficient with angle of attack.

Figure 4.- Concluded.





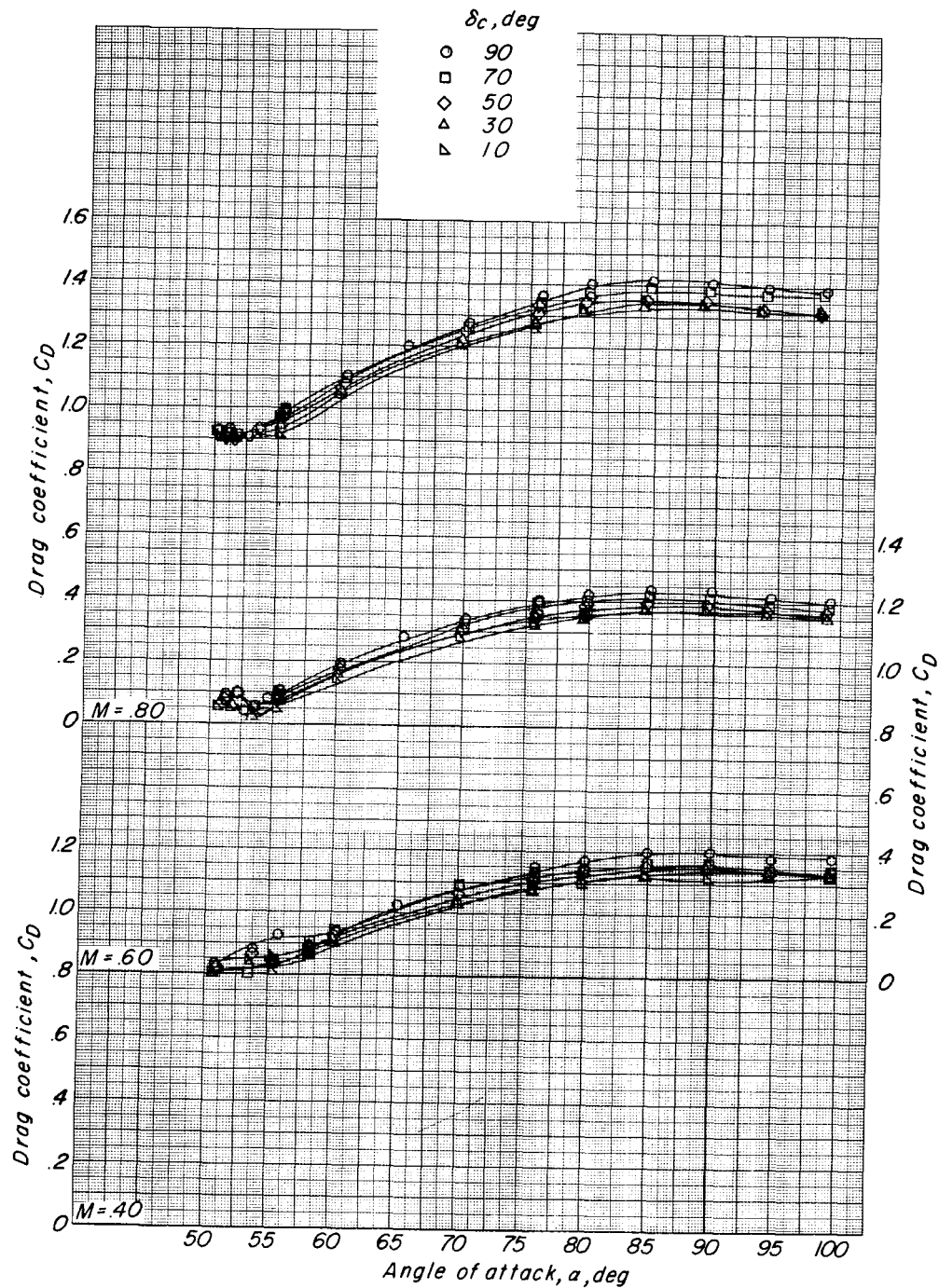
(a) Variation of lift coefficient with angle of attack.

Figure 5.- Effects of deflecting the fuselage nose control tab on the longitudinal stability and control characteristics of the basic  $73^\circ$  delta-wing configuration  $W_1H_1C_1$ .  $\Gamma_h = 0^\circ$ ;  $\delta_f = 0^\circ$ .

# UNCLASSIFIED

CONFIDENTIAL

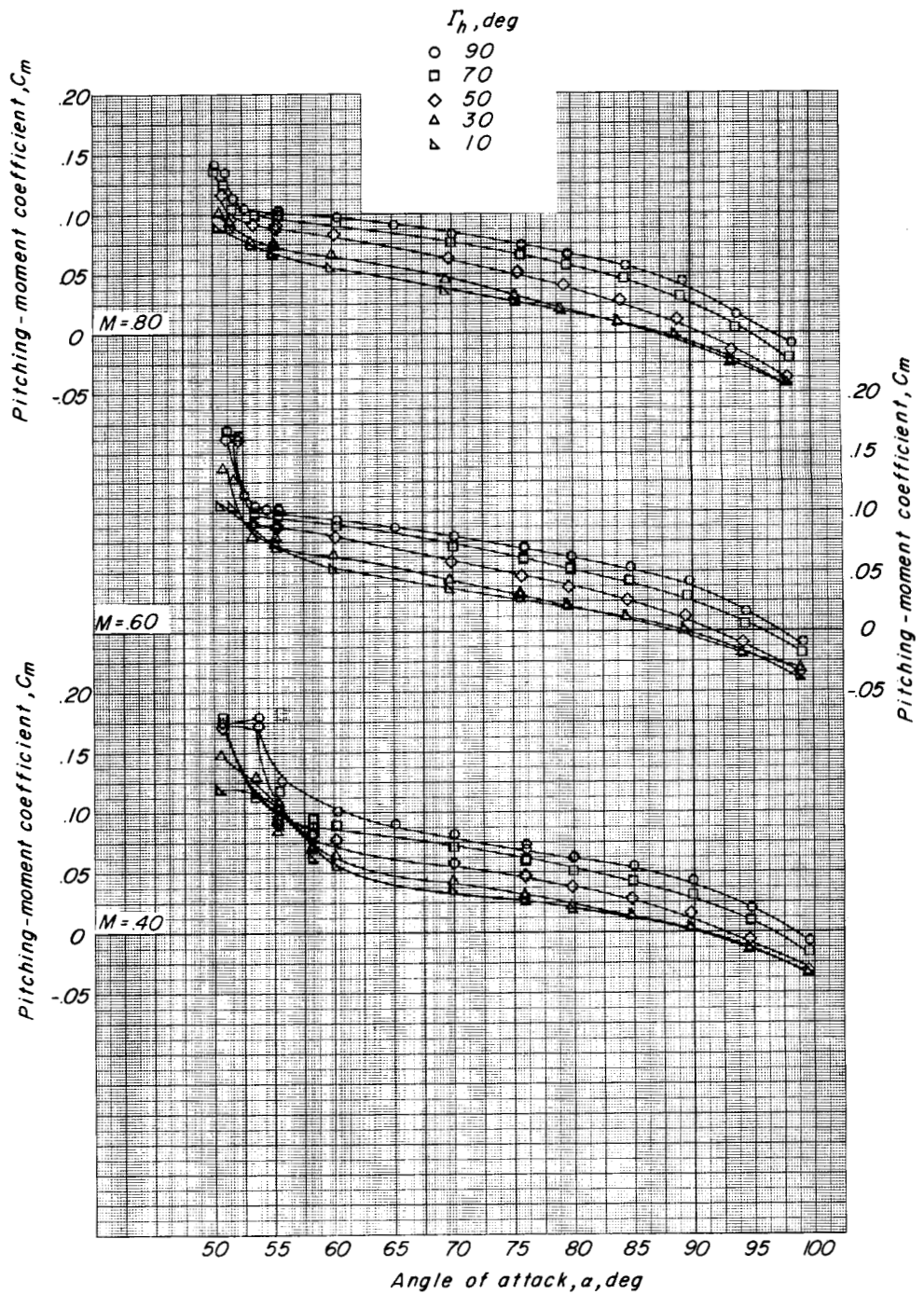
17



(b) Variation of drag coefficient with angle of attack.

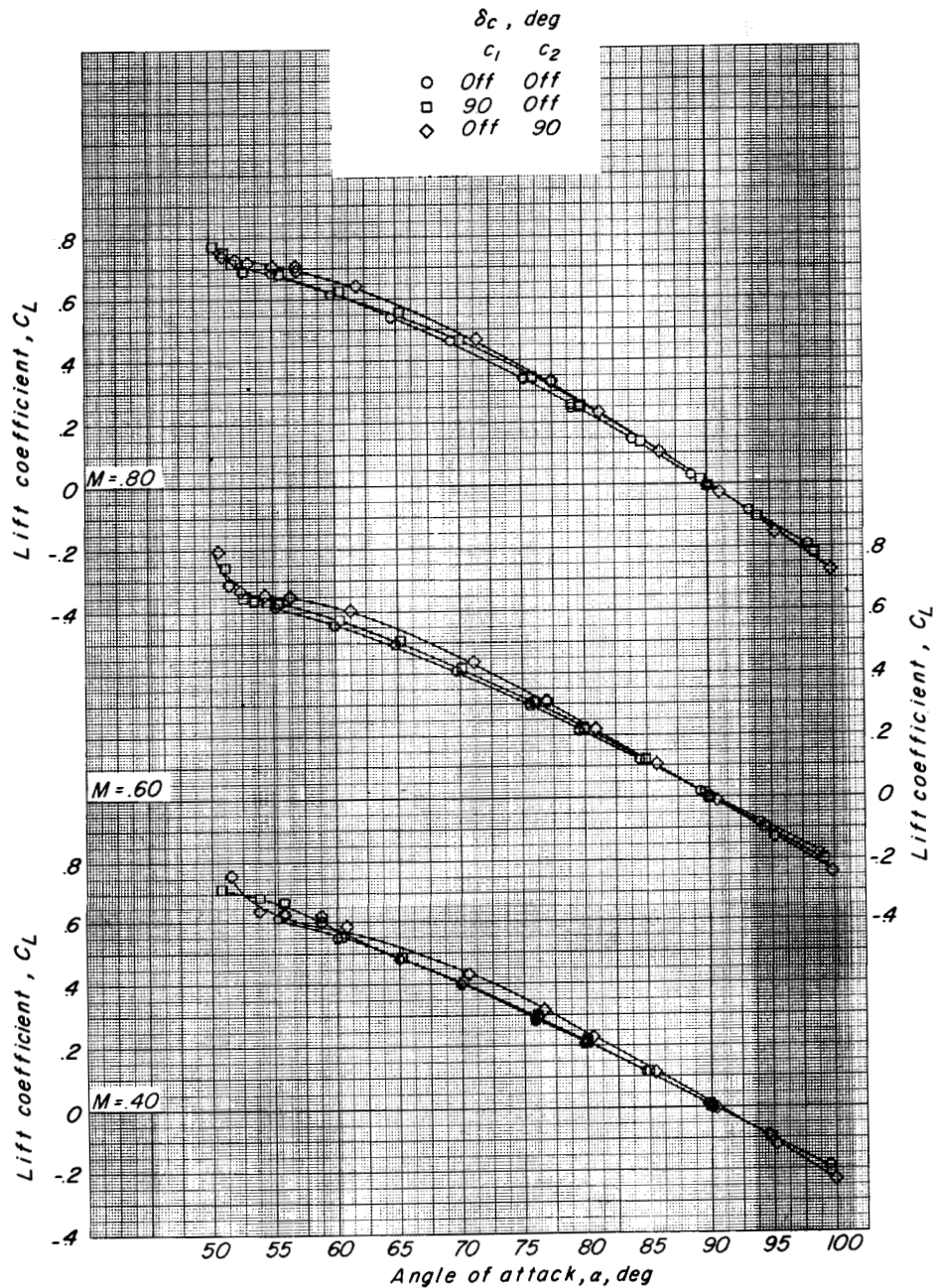
Figure 5.- Continued.

CONFIDENTIAL



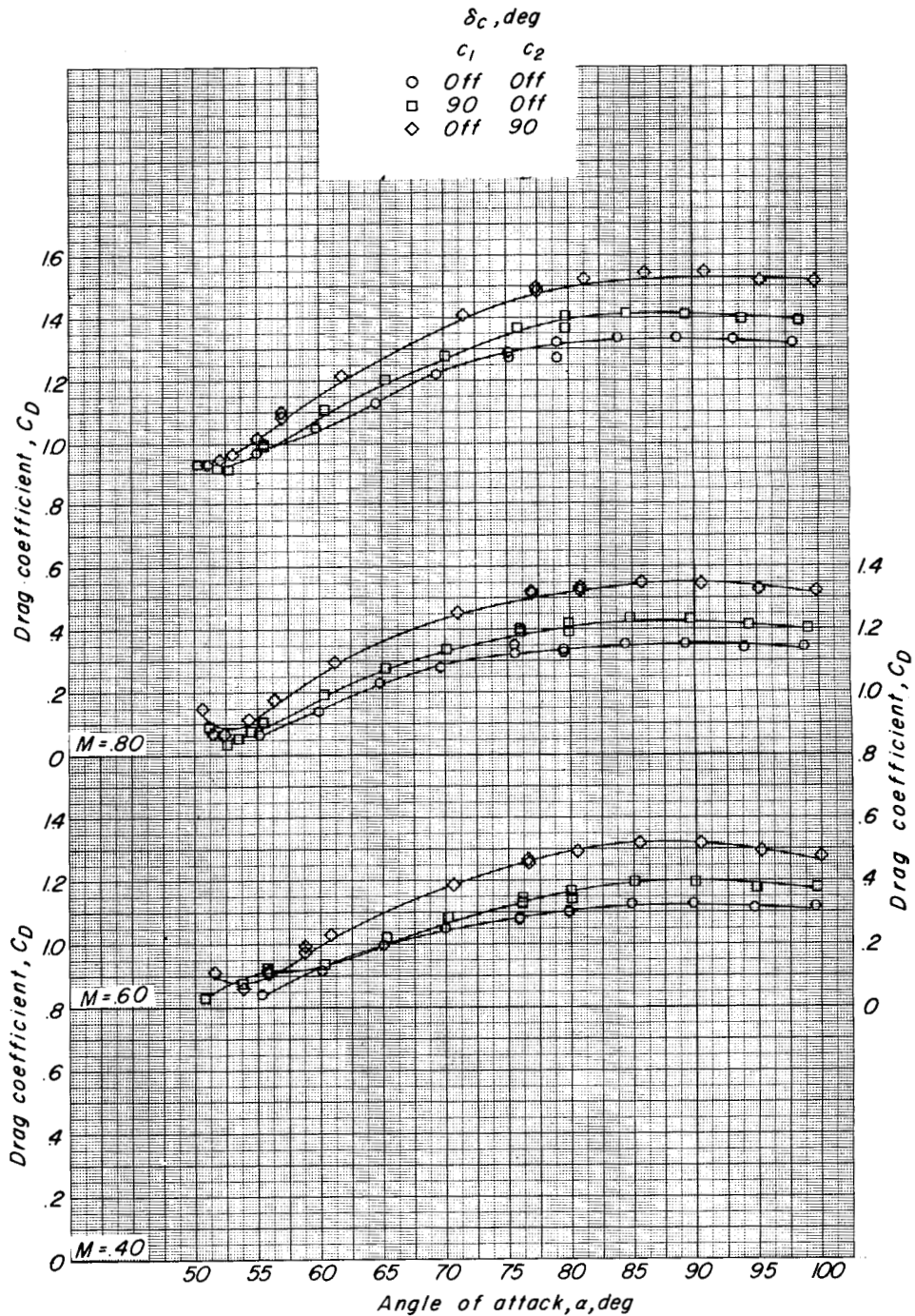
(c) Variation of pitching-moment coefficient with angle of attack.

Figure 5.- Concluded.



(a) Variation of lift coefficient with angle of attack.

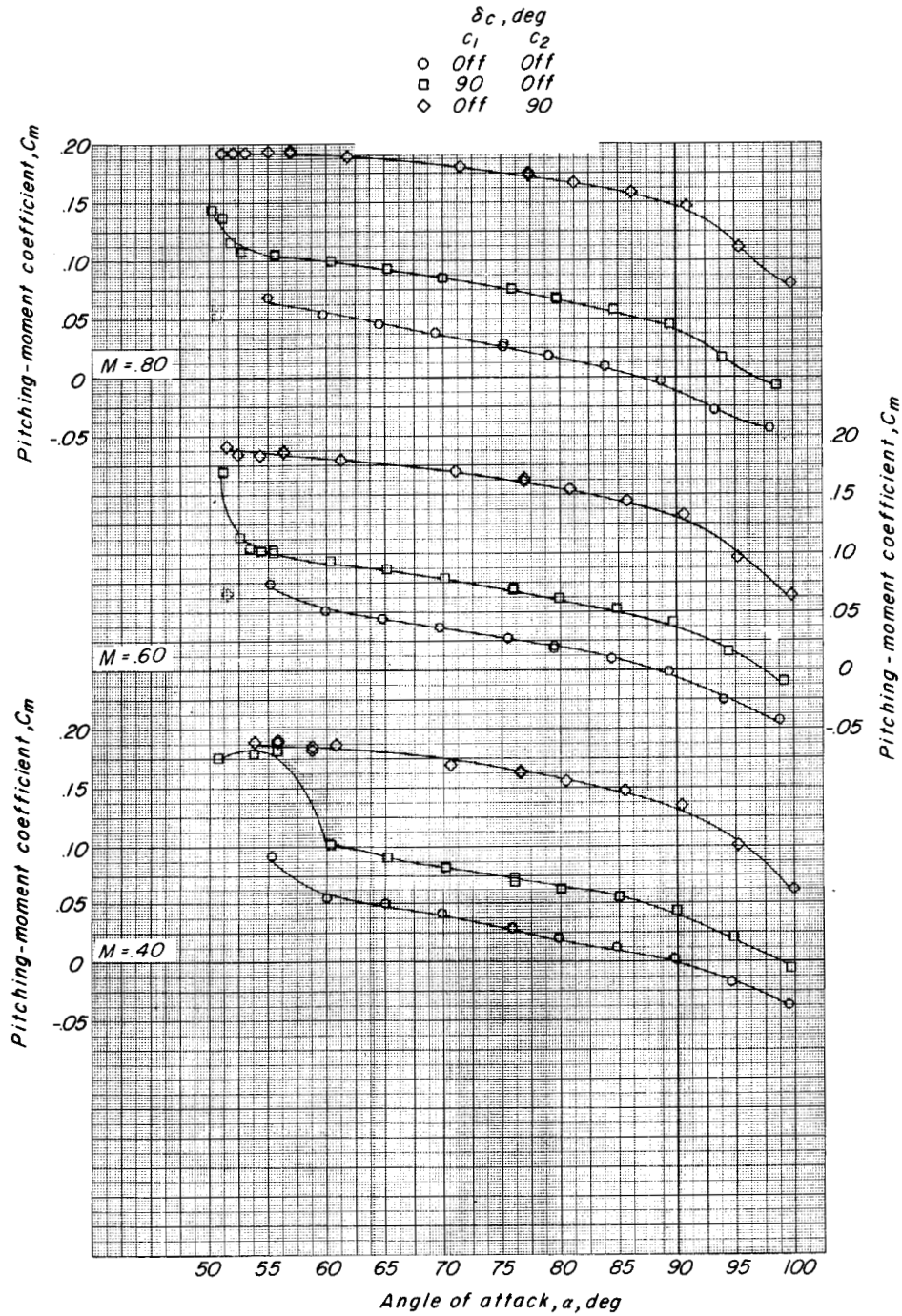
Figure 6.- Effects of size of fuselage nose control tab on the longitudinal stability and control characteristics of the basic  $73^\circ$  delta-wing configuration  $W_1H_1$ .  $\Gamma_h = 0^\circ$ ;  $\delta_f = 0^\circ$ .



(b) Variation of drag coefficient with angle of attack.

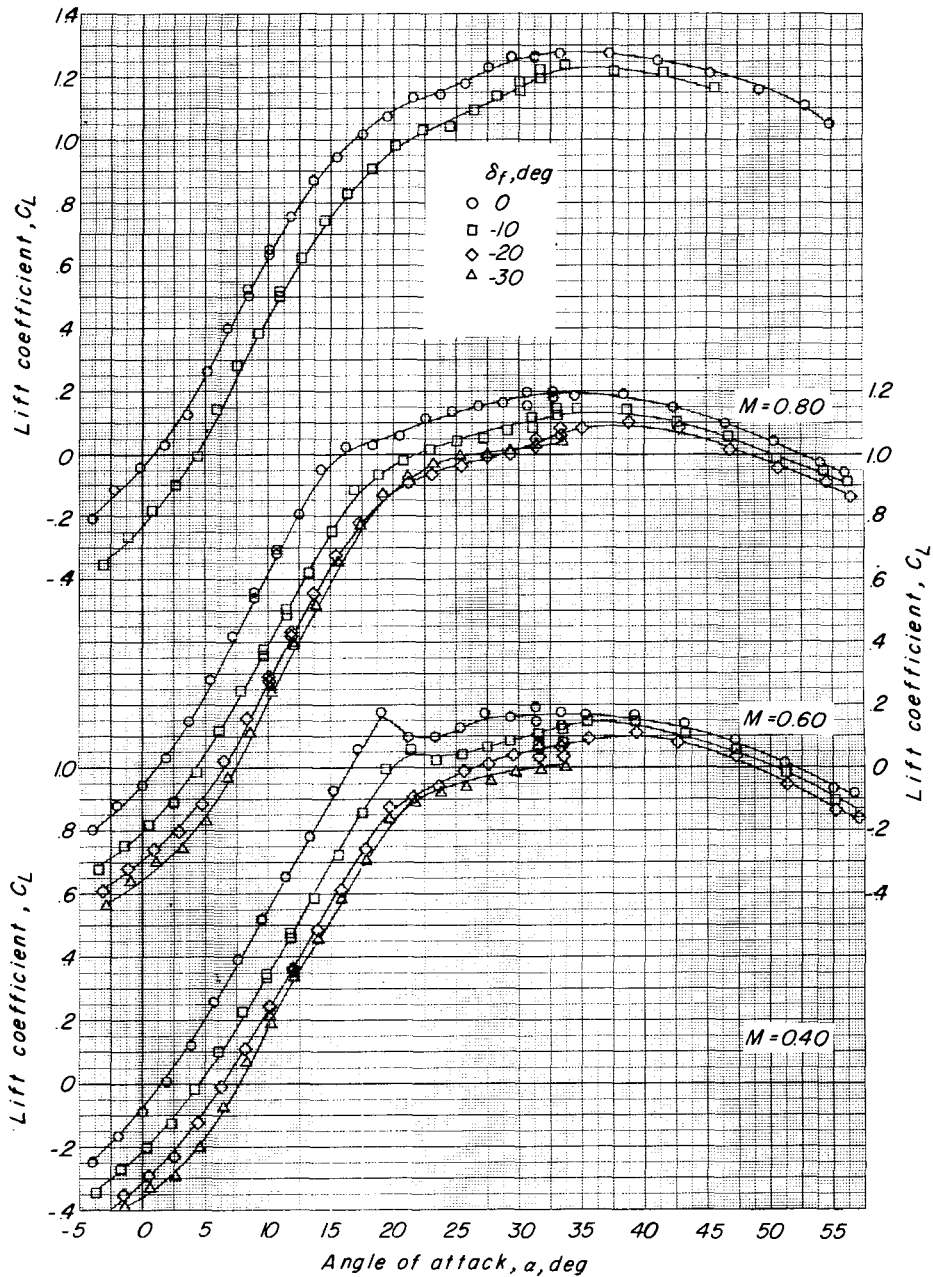
Figure 6.- Continued.





(c) Variation of pitching-moment coefficient with angle of attack.

Figure 6.- Concluded.



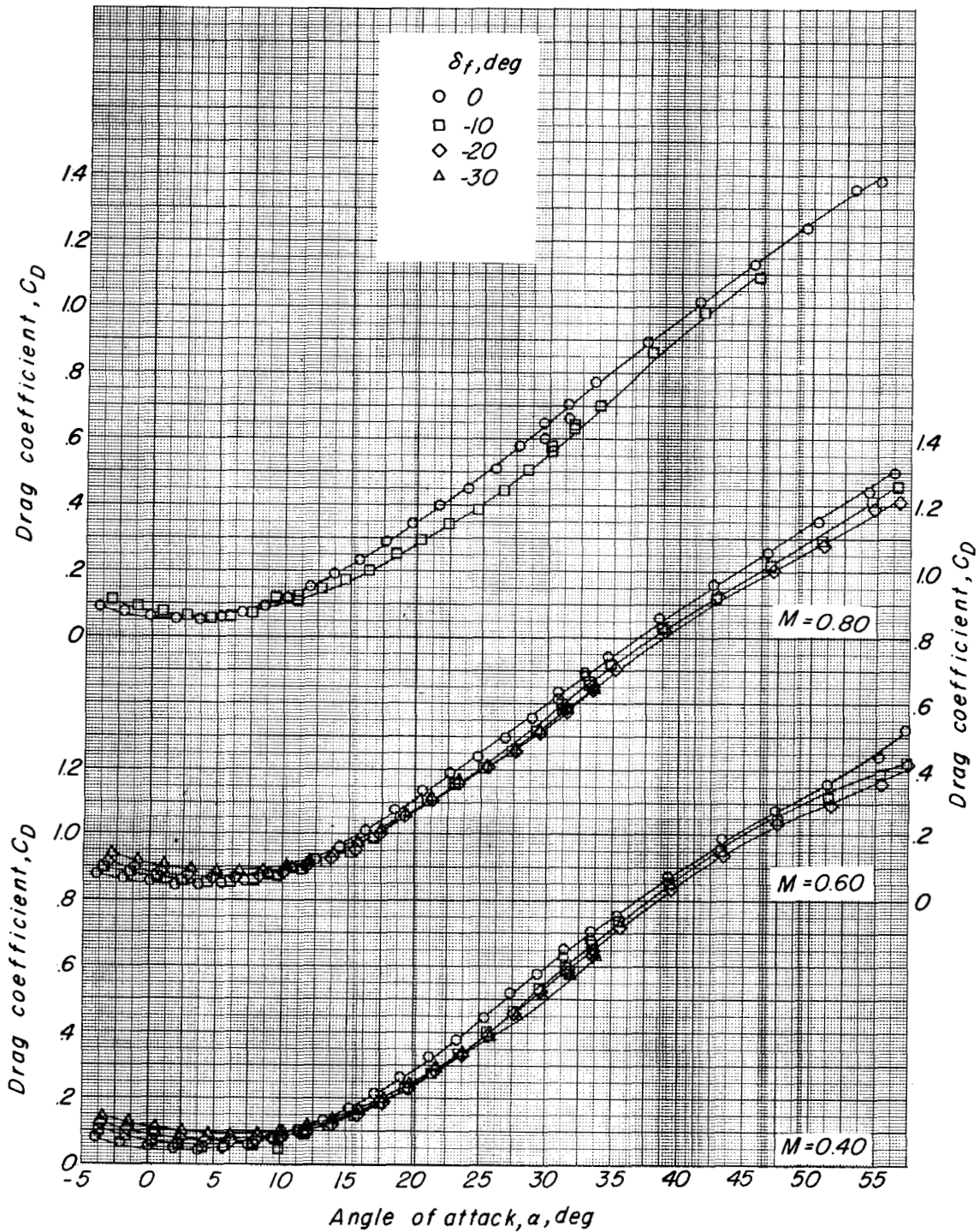
(a) Variation of lift coefficient with angle of attack.

Figure 7.- Effects of deflection of trailing-edge flap of basic wing-tip panel on the longitudinal stability and control characteristics of the basic  $73^\circ$  delta-wing configuration  $W_1H_1$ .  $\Gamma_h = 90^\circ$ ; nose control off.

UNCLASSIFIED

CONFIDENTIAL

23

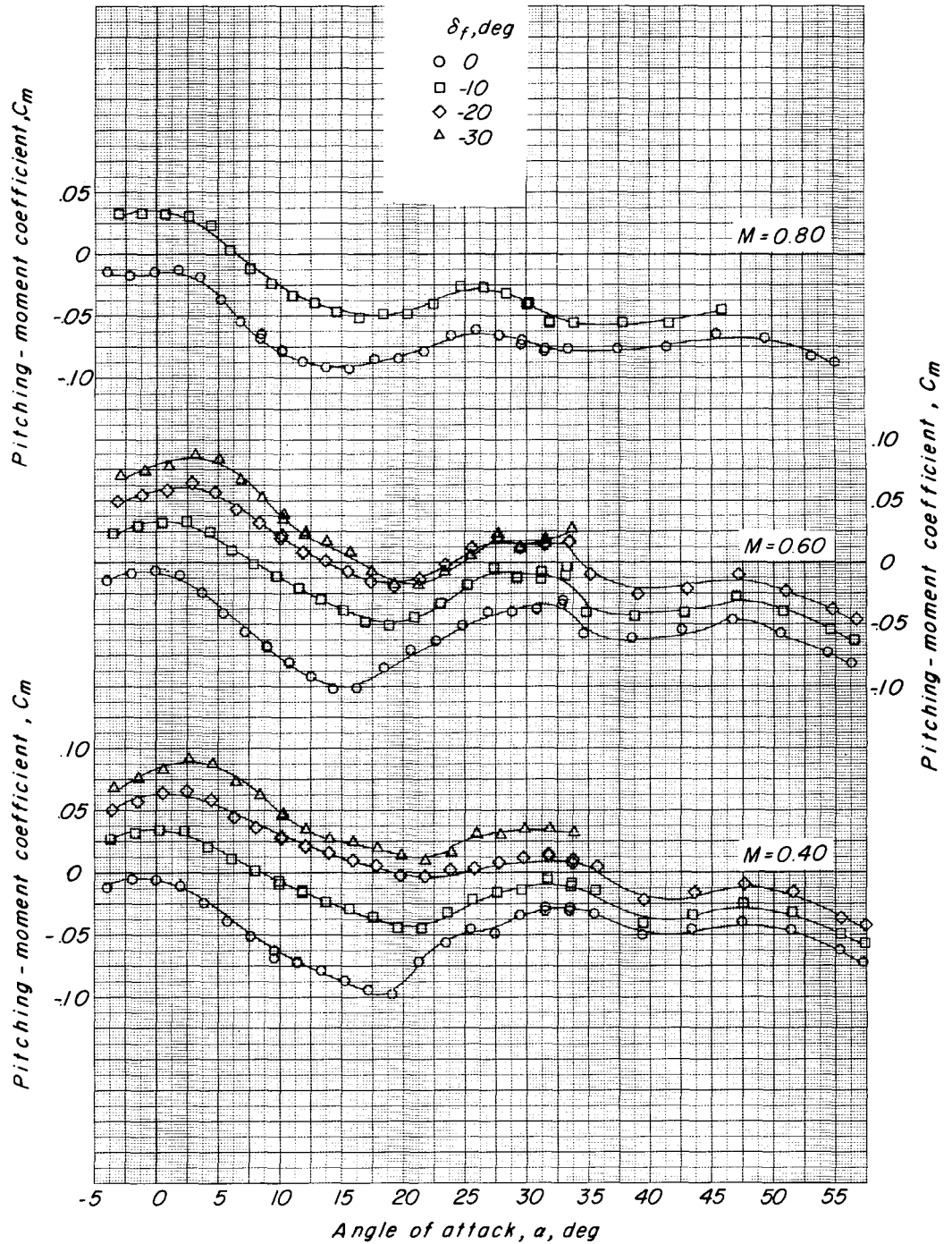


(b) Variation of drag coefficient with angle of attack.

Figure 7.- Continued.

CONFIDENTIAL





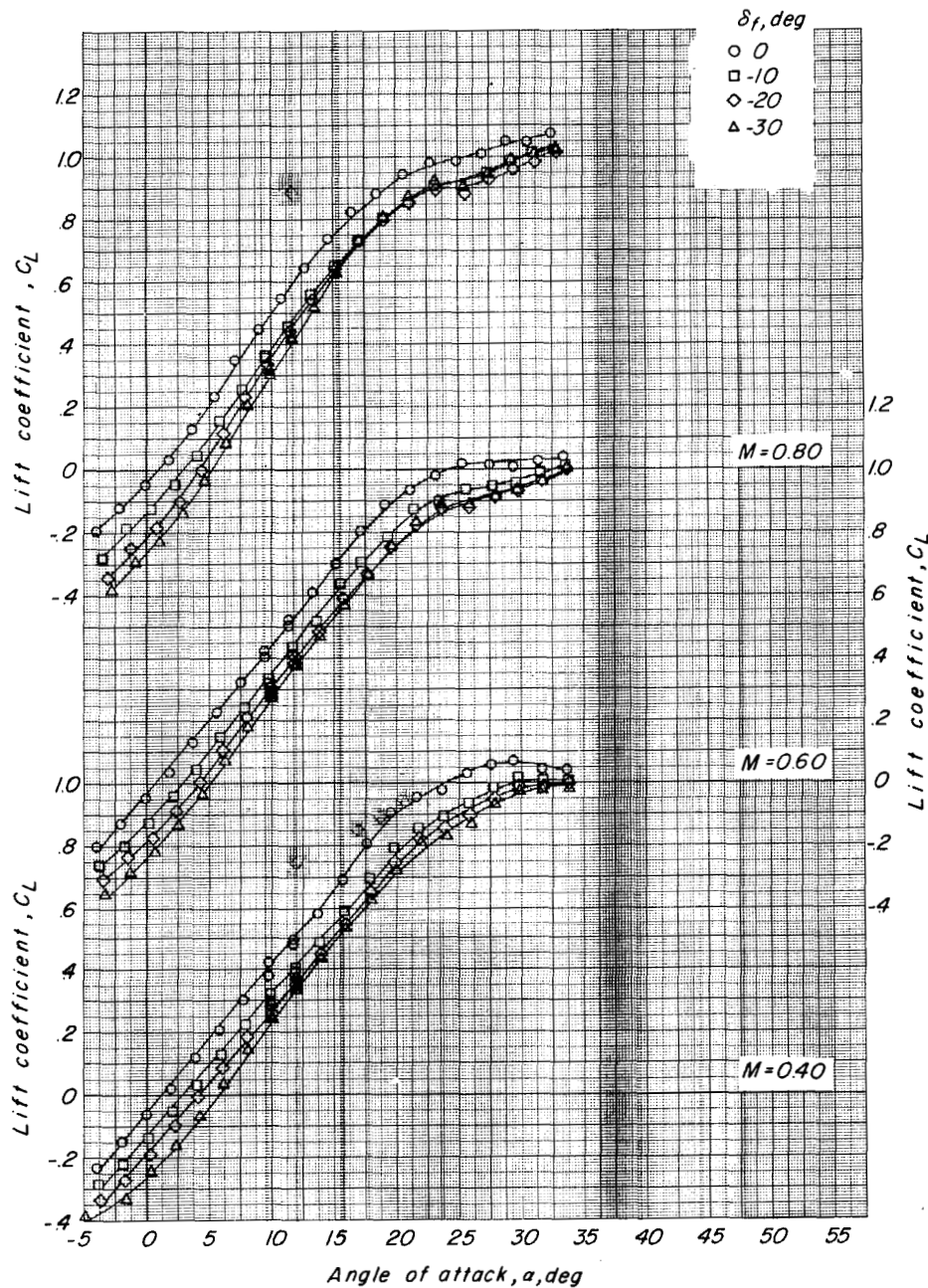
(c) Variation of pitching-moment coefficient with angle of attack.

Figure 7.- Concluded.

UNCLASSIFIED

CONFIDENTIAL

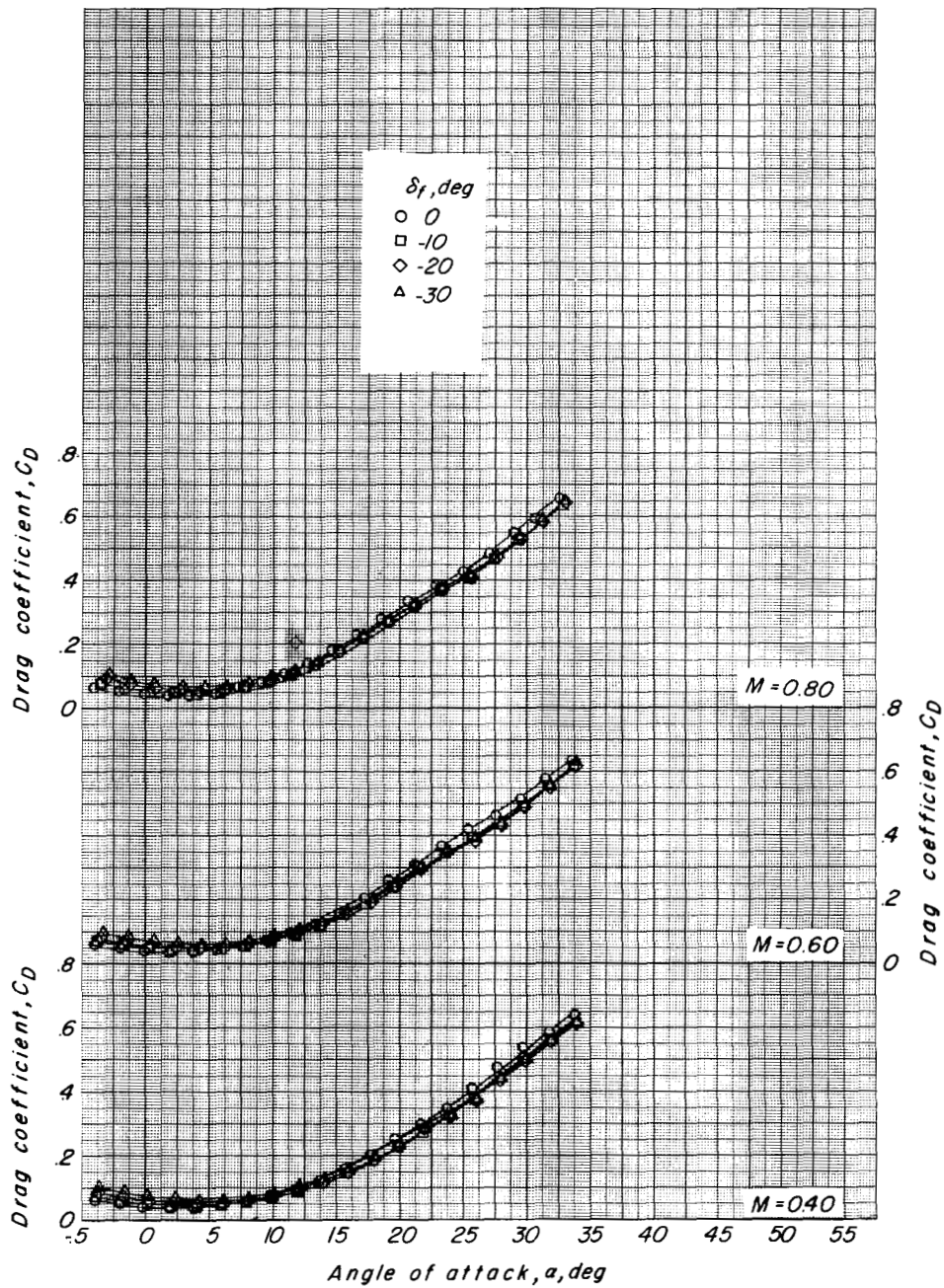
25



(a) Variation of lift coefficient with angle of attack.

Figure 8.- Effects of deflection of trailing-edge flap of modified wing-tip panel on the longitudinal stability and control characteristics of the basic  $73^\circ$  delta-wing configuration  $W_1H_2$ .  $\Gamma_h = 90^\circ$ ; nose control off.

CONFIDENTIAL



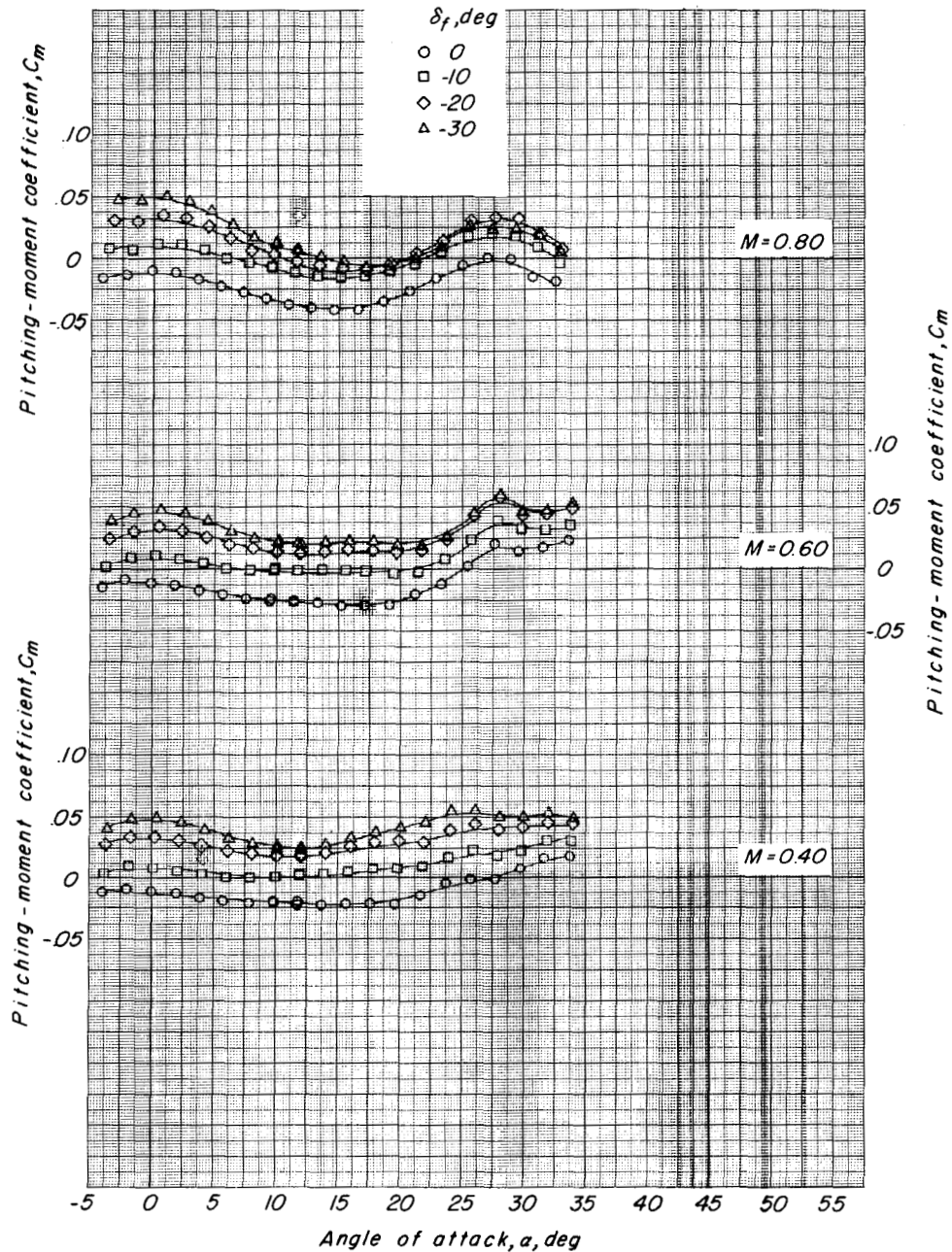
(b) Variation of drag coefficient with angle of attack.

Figure 8.- Continued.

UNCLASSIFIED

CONFIDENTIAL

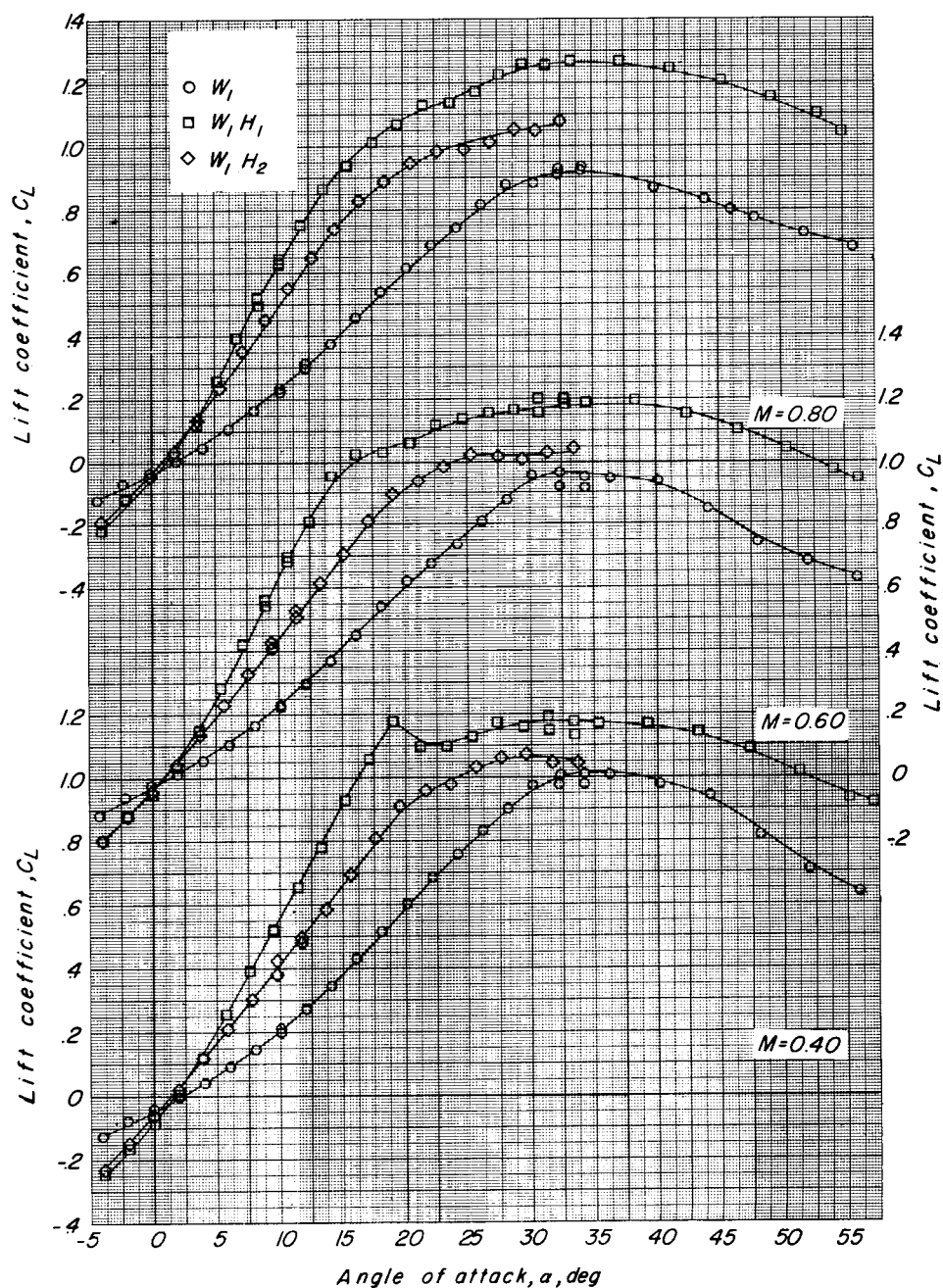
27



(c) Variation of pitching-moment coefficient with angle of attack.

Figure 8.- Concluded.

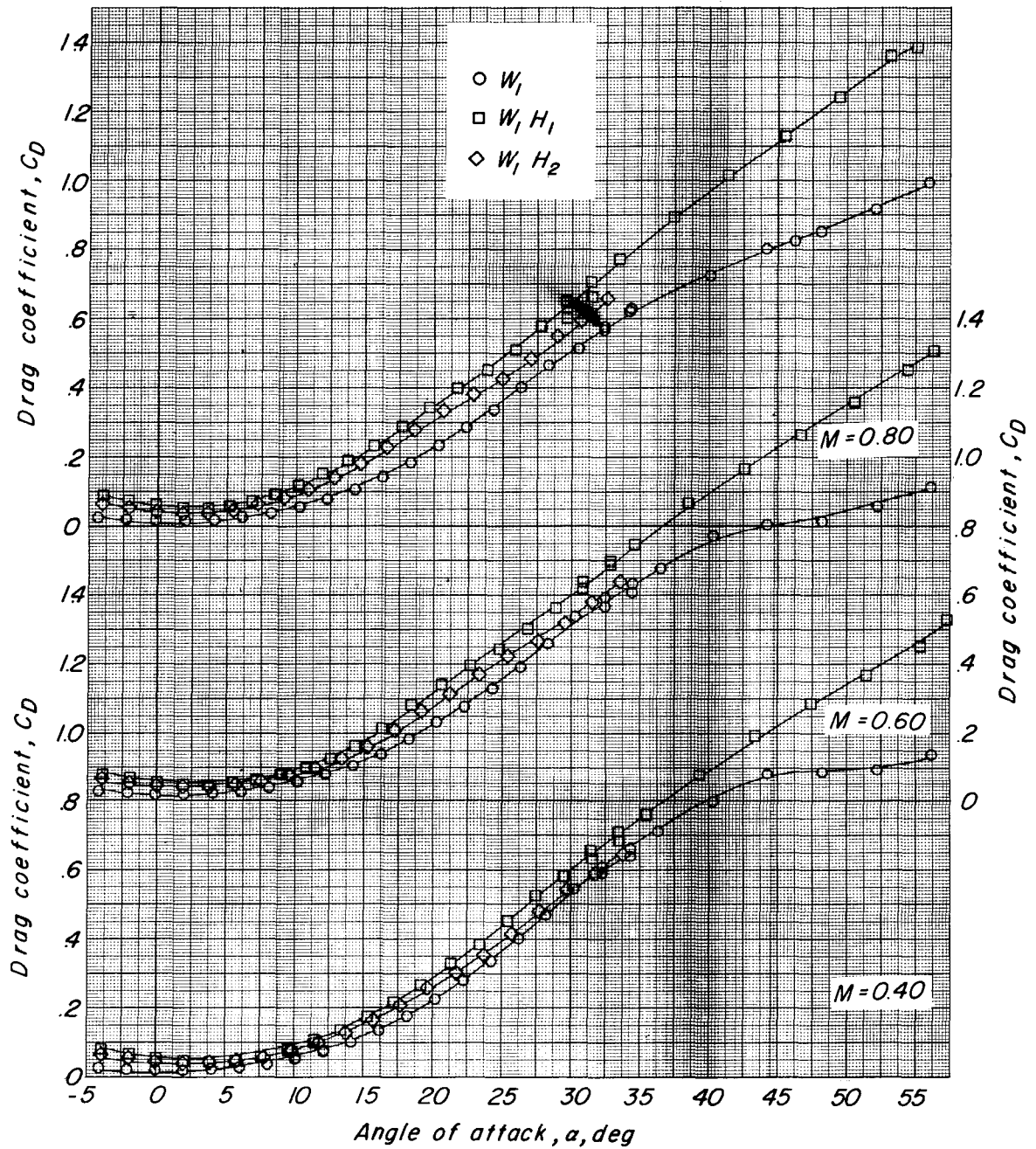
CONFIDENTIAL



(a) Variation of lift coefficient with angle of attack.

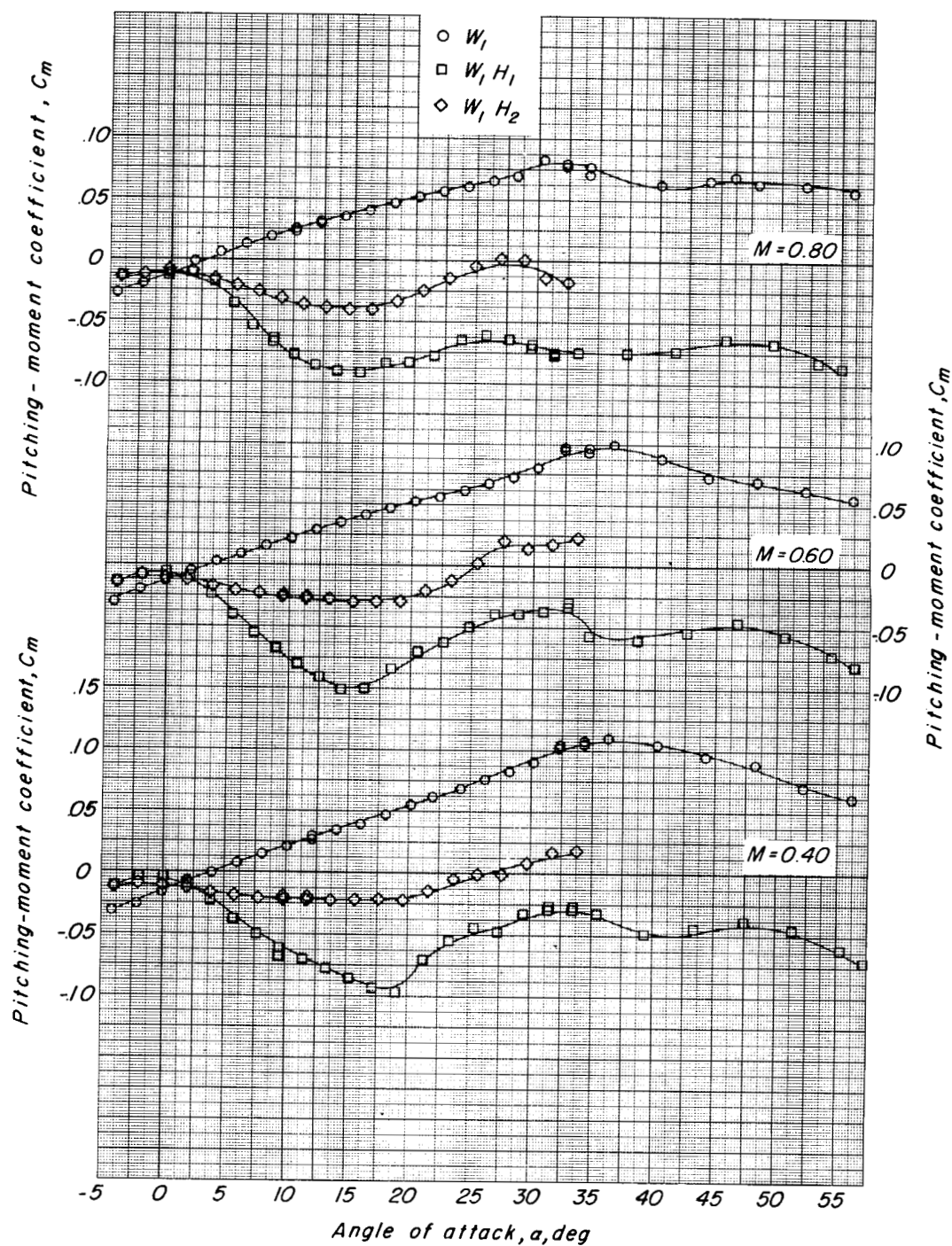
Figure 9.- Comparison of wing-tip panel size on the longitudinal stability characteristics of the basic  $73^\circ$  delta wing.  $\Gamma_h = 90^\circ$ ;  $\delta_f = 0^\circ$ ; nose control off.





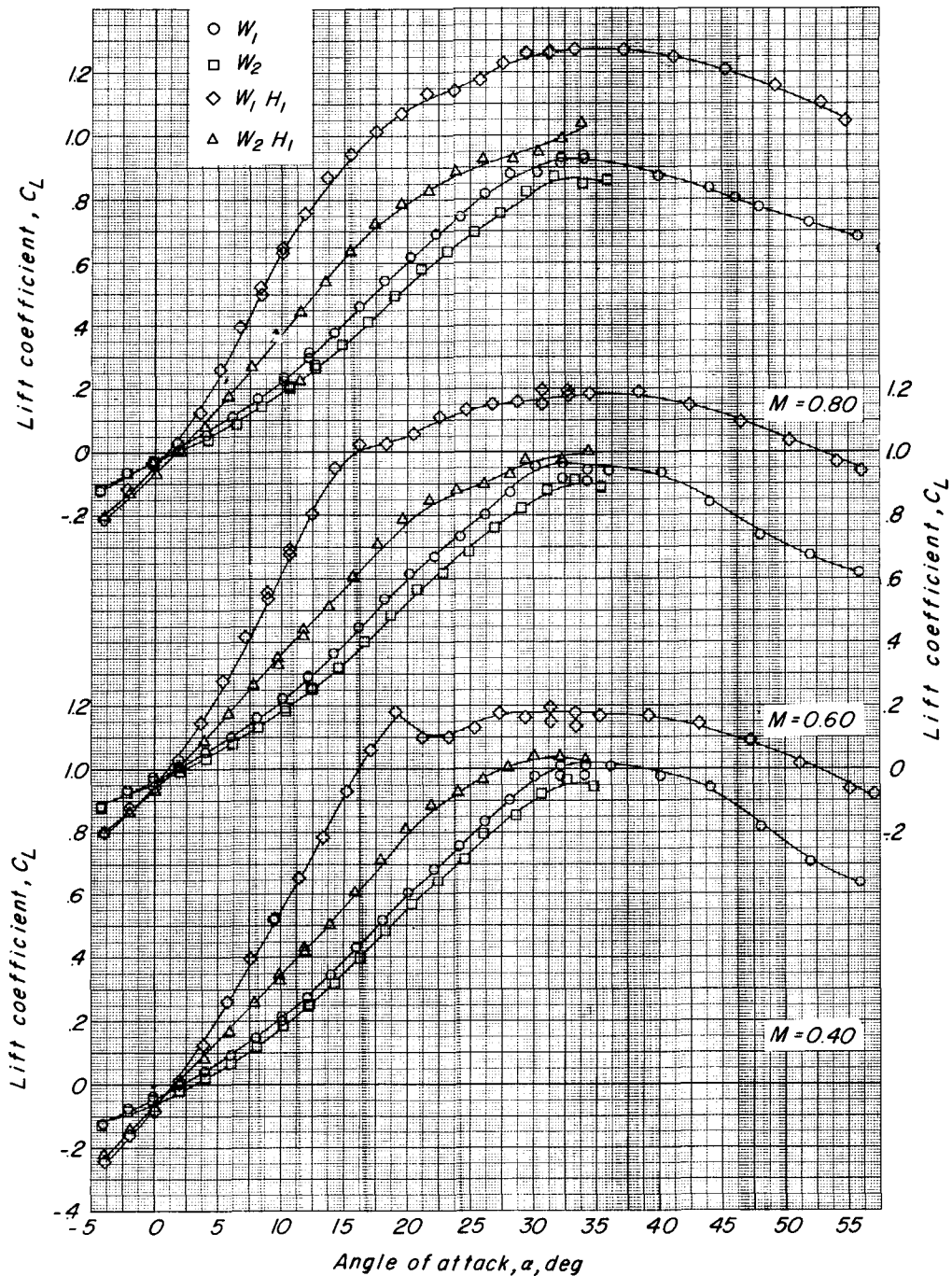
(b) Variation of drag coefficient with angle of attack.

Figure 9.- Continued.



(c) Variation of pitching-moment coefficient with angle of attack.

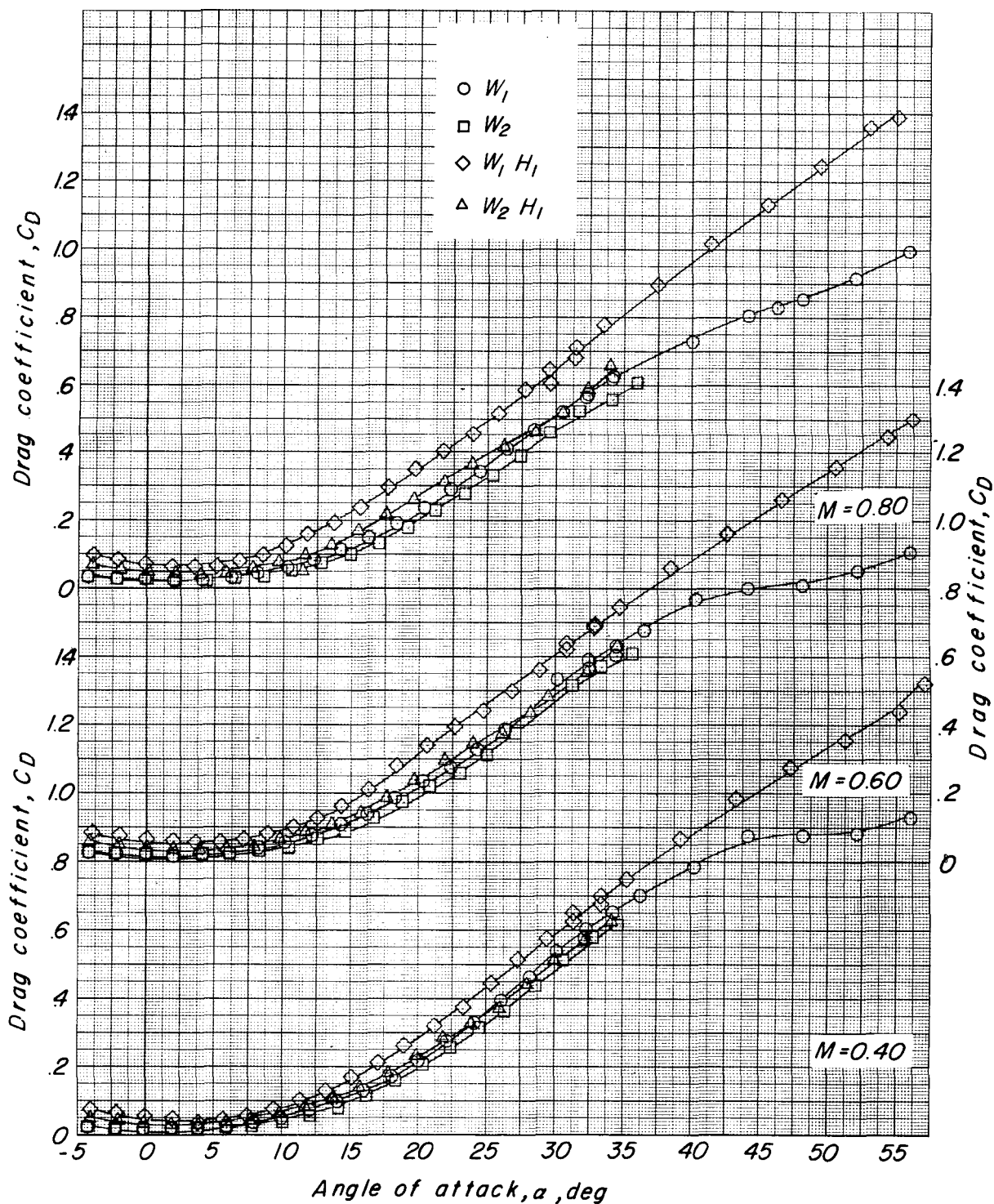
Figure 9.- Concluded.



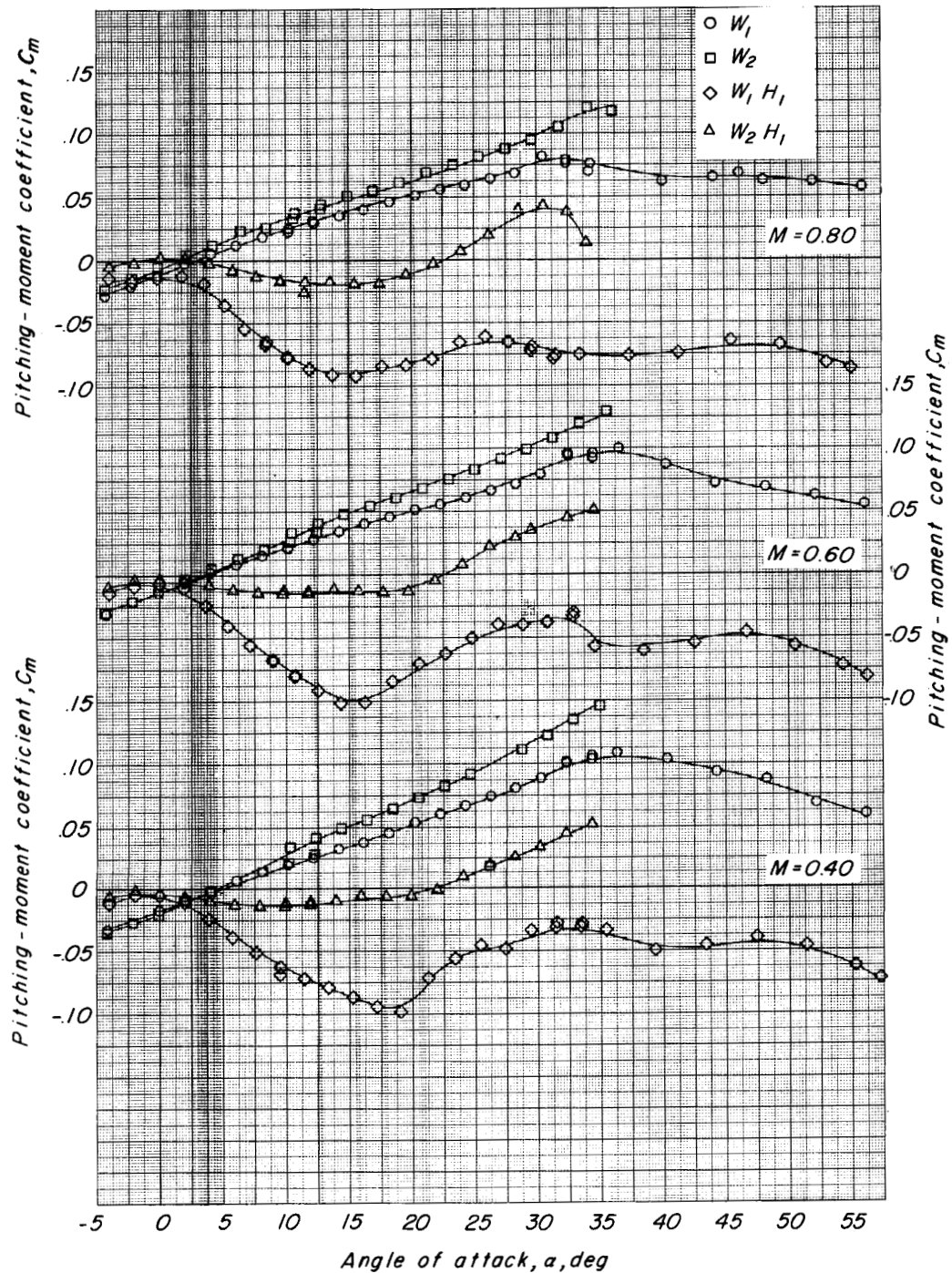
(a) Variation of lift coefficient with angle of attack.

Figure 10.- Comparison of the longitudinal stability characteristics of the basic  $73^\circ$  delta wing and the cranked delta wing, with and without the basic wing-tip panels.  $\Gamma_h = 90^\circ$ ;  $\delta_f = 0^\circ$ ; nose control off.





(b) Variation of drag coefficient with angle of attack.



(c) Variation of pitching-moment coefficient with angle of attack.

Figure 10.- Concluded.